Improved Computations of the Voltage Collapse Point Using the P-Index

By

Siddig Ali Elamin Mohammed

Abdelrahman A. Karrar
Associate Professor of Electrical Engineering
Committee Chair

Ahmed H. Eltom
Professor of Electrical Engineering
Committee Member

Gary L. Kobet
Adjunct Professor of Electrical Engineering
Committee Member

Raga Ahmed
Assistant Professor of Electrical Engineering
Committee Member

Improved Computations of the Voltage Collapse Point Using the P-Index

By

Siddig Ali Elamin Mohammed

A Thesis Submitted to the Faculty of the University of
Tennessee at Chattanooga in Partial
Fulfillment of the Requirements of the Degree of
Master of Science: Engineering

The University of Tennessee at Chattanooga
Chattanooga, Tennessee

December 2018

ABSTRACT

Online voltage stability assessments of power systems are important to ensure reliability and security. Over the years, many voltage monitoring indices have been documented in the literature. These indices are designed to quantify proximity to voltage collapse. However, they all have inaccuracies when predicting the voltage collapse point. A recent research project resulted in a new robust voltage stability monitoring tool called the P-index. A method that utilizes linear approximation of Voltage-Load relationship was introduced alongside the P-index, providing enhanced precision compared to most recognized indices. However, this method generates a high level of inaccuracy because the actual Voltage-Load behavior in general is non-linear, but rather more complex. This study proposed two new models that take into account the nonlinearity of Voltage-Load relationship, providing an enhanced representation of its complexity. Moreover, these models have a higher accuracy than the linear method in predicting voltage collapse points.

TABLE OF CONTENTS

LIST OF TABLES

LIST OF FIGURES

CHAPTER 1

INTRODUCTION

1.1 Overview

The voltage stability area and voltage collapse problems have been a major concern for the power industry because several major blackouts in recent years were considered a consequence of voltage instability. Voltage instability problems generally arise when the system is unable to meet reactive power demand due to a lack of sufficient reactive power resources. One currently used method to prevent voltage collapse uses online voltage monitoring tools to detect voltage instability and make corrective actions before the system enters critical condition. However, accurately predicting the voltage collapse point in an actionable timeframe remains a challenging task.

1.2 Problem Statement

In the last three decades, many voltage stability indices have been proposed in the literature. The main purpose of all these indices is to quantify the distance to voltage collapse point in terms of loading multipliers. However, they all show high inaccuracies when calculating the voltage collapse point. A voltage stability index named the P-index was introduced recently to the literature. This index provided a robust detection of voltage instability and fast prediction of

voltage collapse point. However, this index, like its predecessors, still lacks sufficient accuracy due to the assumptions made in modeling the voltage-loading behavior.

1.3 Objective

The main objective of this study is to improve the model used to predict voltage collapse point using the P-index. The new model proposed in this study took into account the nonlinearity of voltage-load behavior that was assumed in the original P-index study. The resulting improved model is designed to provide higher accuracy of prediction over other voltage stability indices.

1.4 Thesis Layout

The remainder of this thesis is organized as follows:

- Chapter 2: this chapter provides an overview of the literature on different voltage stability analysis tools.
- Chapter 3: this chapter introduces the concepts behind the improved models along with the derivation of their formulas.
- Chapter 4: this chapter presents simulation results when applying the improved methods on different test systems. Moreover, comparison with other robust voltage stability analysis tools is presented.
- Chapter 5: this chapter concludes the contributions and findings of this work. Furthermore, it provides some suggestions and recommendations for further research work.

CHAPTER 2

LITERATURE REVIEW

2.1 Voltage Stability

Voltage stability is defined in this study, as proposed by an IEEE/CIGRE joint task force, as “The ability of power system to maintain steady voltages at all buses in the system after being subjected to a disturbance from a given initial operating point. The system state enters the voltage instability region when a disturbance or an increase in load demand or alteration in system state results in an uncontrollable and continuous drop in system voltage” [1].

Voltage collapse is a system instability that involves multiple components of the system and may spread to the entire system, at which point it is termed a “blackout”. Voltage collapse mostly occurs in highly loaded system. The main factor that leads to voltage instability is the lack of sufficient reactive power resources where the system cannot meet the demand. From that point, voltage continues to drop as the load grows until the point where voltage-sensitive protection devices pick-up and start to operate leading to uncontrolled outages. These outages may spread throughout the system, leading to a total blackout.

Voltage instability has been the chief cause of several blackouts. The major blackout in the United Stated and Canada on August 14, 2003 is a famous example of voltage instability: the largest blackout ever of the North American power grid. The blackout affected an estimated 50 million people, disconnecting more than 70,000 megawatts of load [2]. Other large-scale voltage

stability-related incidents include the power failure in Eastern Denmark and Southern Sweden on September 23, 2003 [3], and the Brazilian Blackout of 2009 [4].

Voltage stability has gained a large amount of research attention because of the important role it played in the afore-mentioned blackouts. Researchers started investigating voltage stability, and efforts today are still being put towards finding ways to monitor the voltage to detect and prevent any abnormalities that could lead to catastrophic events.

A parallel line of research that has been around since the 1980s is concerned with monitoring and predicting the distance to voltage collapse in terms of load multipliers. In this field of study, a new term arose and is known as "voltage indices". A voltage index is a voltage stability indicator that shows how close the system is to voltage collapse. One of the earliest voltage indices is the L-index that was developed in 1988, and one of the recent indices is the P-index that was developed in 2018. Between these two, many voltage indices were introduced in the literature. These indices differ in system components that they are based on. For instance, some indices are line based while others are bus based. Moreover, they differ in the application that they are intended for. Some of them are intended for offline voltage assessment for design purposes, while others are claimed to be suitable for online voltage stability analysis. The next sections include an overview of the voltage stability analyzing tools and some of the important indices in the literature.

2.2 P-V and Q-V Analysis

P-V and Q-V curves are amongst the most fundamental power flow-based static analysis tools. P-V curves, also known as nose curves, show the relationship between the active power loading and the voltage of a particular bus. It is obtained by increasing the load of the system in steps while observing the corresponding voltage at some critical buses, and then plotting the

voltage against the load. However, when approaching the voltage collapse point, voltage decreases drastically with the slightest increase in load. The load flow Jacobian matrix becomes singular at that point and conventional load flow is unable to find a solution. To overcome this problem, power flow equations are reformulated to perform what is known as the continuation power flow.

A continuation power flow consists of prediction and correction steps. From a known base solution, a tangent predictor estimates next solution for a step of load increase. The exact solution is then obtained by performing a conventional power flow in a corrector step. After that, a new prediction is made for another increase in load based on the new tangent vector. Then corrector step is applied. The predictor-corrector process is performed until the critical point is reached. At the critical point the tangent vector is zero [5]. Figures 2.1 and 2.2 illustrate the P-V curves and the Predictor-Corrector scheme, respectively.

The P-V curves consist of two regions. The upper region is the stable operating region where an increase in load results in a drop in voltage. The lower region is the unstable operating region where an increase in load results in an increase the voltage.

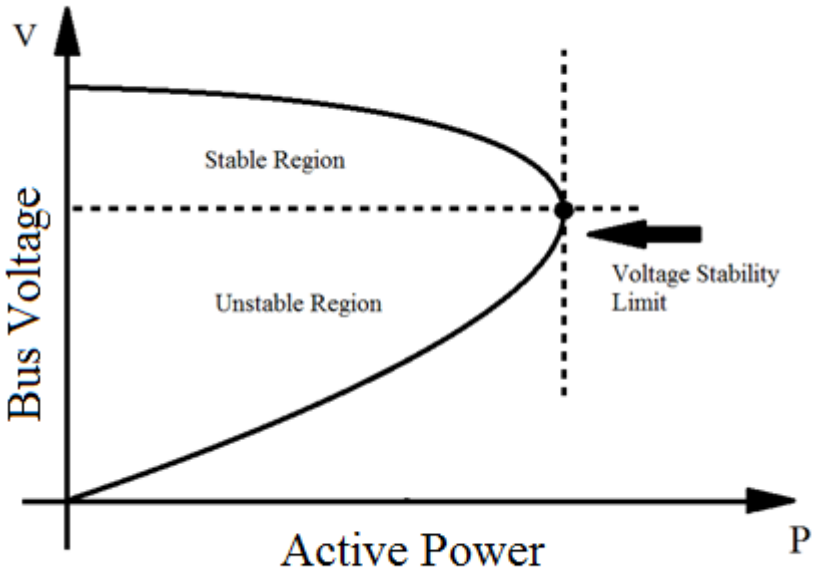

Figure 2.1 Active power loading relationship with bus voltage (P-V curve)

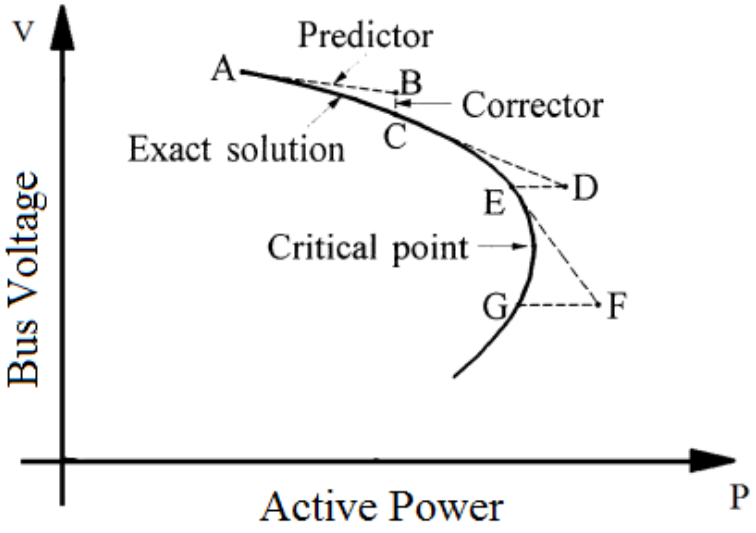

Figure 2.2 Continuation power flow predictor-corrector scheme

The second tool for analyzing voltage stability is using Q-V curves. Similar to P-V curves, Q-V curves show the change in voltage with respect to a change in the reactive power injection into a particular bus as illustrated in Figure 2.3. Furthermore, Q-V curves show two operation regions: the right-hand side of the graph corresponds to a stable operating region where an increase in the reactive power injection results in an increase in voltage. The left-hand side of the graph is the unstable region, where an increase in the reactive power injection results in a drop in voltage. The lowest point of the Q-V curve is the voltage collapse point. The rate of change in voltage with respect to Q is equal to zero.

P-V and Q-V curves are useful in estimating the distance to voltage collapse. However, these two methods have their drawbacks. Both methods are not suitable for online voltage stability limit estimation as they require a large number of mathematical operations. This is time consuming, especially for systems with large number of buses, where numerous load flows must be executed.

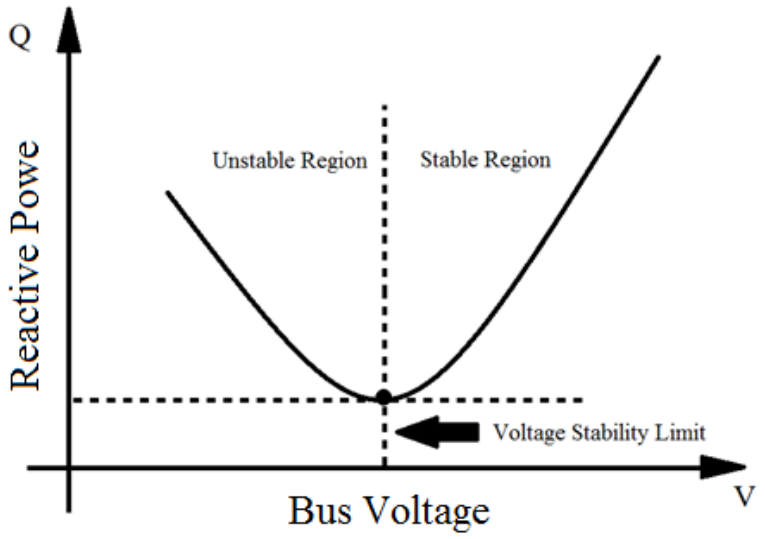

Figure 2.3 Reactive power injection relationship with bus voltage (Q-V curve)

2.3 Modal Analysis

Modal analysis is another static approach for voltage stability analysis. Presented by Gao, Morisson and Kundur in 1992 [6], this method utilizes the system eigenvalues to estimate proximity to voltage collapse. Moreover, the method identifies the elements of the power system that contribute the most towards voltage instability, e.g. critical load buses, branches and generators.

Eigenvalues and eigenvectors are obtained from the system's reduced Jacobian matrix.

Given the following power flow equation:

$$\begin{bmatrix}\Delta P\\ \Delta Q\end{bmatrix} = \begin{bmatrix}J_{P\delta} & J_{PV}\\ J_{Q\delta} & J_{QV}\end{bmatrix}\begin{bmatrix}\Delta\delta\\ \Delta V\end{bmatrix} \quad 2.1$$

Let $\Delta P = 0,$ then:

$$\Delta Q = J_R \cdot \Delta V \quad 2.2$$

Where:

$$J_R = \left[J_{QV} - J_{Q\delta} \cdot J_{P\delta}^{-1} \cdot J_{PV}\right] \quad 2.3$$

If J_R is defined as:

$$J_R = \xi \Lambda \eta \quad 2.4$$

Where:

$\xi =$ right eigenvector matrix of J_R

$\eta =$ left eigenvector matrix of J_R

$\Lambda =$ diagonal eigenvalue matrix of J_R

From 2.4:

$$J_R^{-1} = \xi \Lambda^{-1} \eta \qquad 2.5$$

Substituting 2.2 in 2.5, and manipulating the equations give:

$$\Delta V = \sum_i \frac{\xi_i \eta_i}{\lambda_i} \Delta Q \qquad 2.6$$

The i^{th} mode of Q-V response is defined by the eigenvalue λ_i and the corresponding right and left eigenvectors ξ_i and η_i.

The modal analysis method examines the sign of the eigenvalues to indicate voltage instability. For a positive eigenvalue ($\lambda_i > 0$), the i^{th} modal voltage and the i^{th} modal reactive power variations (ΔV_i and ΔQ_i) are along the same direction and the system is considered voltage stable. On the other hand, a negative eigenvalue ($\lambda_i < 0$) indicates that the i^{th} modal voltage and the i^{th} modal reactive power variations (ΔV_i and ΔQ_i) are along opposite directions and the system is considered voltage unstable. An eigenvalue that has a value of zero ($\lambda_i = 0$) represents the voltage collapse point where any change in the modal reactive power causes an infinite change in the modal voltage.

2.4 Voltage Stability Indicators for Power Systems

A significant number of voltage stability monitoring and assessment indices have been introduced in the literature. A voltage stability index is a scalar magnitude that can be monitored as system parameters change [7]. These indices can explain the two voltage instability fundamental

aspects defined in [1]: proximity to voltage collapse, i.e. how close the system is to voltage instability, and mechanism of voltage instability by pointing out the weak nodes of the system.

Voltage stability indices (VSIs) are classified into two broad categories, Jacobian matrix based VSIs and system variables based VSIs. Jacobian matrix based VSIs can calculate the voltage collapse point and determine the voltage stability margin. The main drawback of Jacobian matrix-based VSIs is the high computation time. Hence, they are not suitable for online voltage instability assessment. On the other hand, system variables-based VSIs use the elements of the admittance matrix and some system variables, e.g. bus voltages or power flow through lines.

Contrary to the Jacobian matrix-based VSIs, these indices require less computation time which makes them attractive for online monitoring. The main disadvantage of these indices is that they cannot accurately estimate the margin. However, they can identify critical lines and buses.

2.4.1 Jacobian Matrix-based VSI

As discussed in Section 2.3, the voltage collapse point is a system loadability limit in which the minimum magnitude of the eigenvalues of the power flow Jacobian matrix is zero. A voltage stability index that uses the minimum singular value of the Jacobian matrix as an indicator of voltage instability was introduced in [8]. This index was unable to predict the accurate voltage collapse point because of the non-linear behavior when approaching the stability limit [7]. Researches tried to avoid this non-linearity problem, and new power flow Jacobian matrix-based indices were proposed such as:

- Test Function [9], which is a function that uses a quadratic model to predict voltage collapse point.
- Second Order Index [10] or index I.

- Tangent Vector [11], which gives information on how system variables (the bus voltage magnitudes and angles) are affected by changing the load multiplier λ.
- V/V0 ratio [12], which is the ratio between the bus voltage V (known from load flow or state estimation studies) and V0 that is obtained by solving load flow for the system at an identical state but with all loads set to zero. This ratio is measured at each node of the system allowing the detection of weak spots.

2.4.2 System Variables-based VSI

The other category of the voltage stability indices is based on direct measurements of the power system, such as bus voltages and elements of the admittance matrix. These indices require less computational efforts which make them suitable for online monitoring and voltage instability assessment.

The system variables-based VSIs are classified in two groups: line stability indices and bus voltage computation indices (or nodal voltage stability indices) [7].

Most of line stability indices are formulated based on the power transmission concept in a single line. These indices include: Lmn index [13], Line Voltage Stability Index (LVSI) [14], LQP-index [15], Fast Voltage Stability Index (FVSI) [16], and Voltage Collapse Point Indicators (VCPI) [17],

Some of the bus voltage computation indices include L index [18], Voltage Collapse Index (VCI) [19], Stability Index (SI) [20], and the recently developed P-index [21].

2.4.2.1 The L index

The L index is a voltage stability indicator that uses information of a normal load flow to predict voltage instability or proximity to voltage collapse. It ranges between 0 (system at no-load condition) and 1 (voltage collapse) [18] .

The L index is based on a hybrid (H) matrix representation of the transmission system with the following set of equations:

$$\begin{bmatrix} V_L \\ I_G \end{bmatrix} = [H] \begin{bmatrix} I_L \\ V_G \end{bmatrix} = \begin{bmatrix} Z_{LL} & F_{LG} \\ K_{GL} & Y_{GG} \end{bmatrix} \begin{bmatrix} I_L \\ V_G \end{bmatrix} \quad 2.7$$

Where:

V_L, I_L = Vectors of voltages and currents at consumer nodes.

V_G, I_G = Vectors of voltages and currents at generator nodes.

$Z_{LL}, F_{LG}, K_{GL}, Y_{GG}$ = submatrices of the H-matrix.

The H matrix can be obtained by partial inversion of the admittance matrix (Y) with exchanging the voltages at the consumer nodes against their currents.

Using the above representation, the L index is defined for any load node j as follows:

$$L_j = \left| 1 + \frac{\underline{V_{0j}}}{\underline{V_j}} \right| \quad 2.8$$

Where:

$$\underline{V_j} = \sum_{i \in L} \underline{Z_{ji}} \cdot \underline{I_j} + \sum_{i \in G} \underline{F_{ji}} \cdot \underline{V_i} \quad 2.9$$

And:

$$\underline{V}_{0j} = -\sum_{i \in G} \underline{F}_{ji} \cdot \underline{V}_i \qquad 2.10$$

As the load at a consumer bus increases, the L index increases until it reaches 1 at the point of voltage collapse. Hence, buses with higher L index are the weakest.

It is worth mentioning that the L index is extended to n-bus system through analogy of a two-bus system. This leads to inaccuracies in estimation as the number of buses increases [21].

2.4.2.2 The P-index

A recent research effort resulted in the development of a new bus-based multi-bus online voltage stability monitoring index named P-index.

This index was based on the observation that a small change in the load (ΔP) is made up of two opposing terms [21]. To explain this concept, consider the two bus system in Figure 2.4.

The load at bus 2 is $P_L + jQ_L$ and the voltage magnitude is *V*. The equivalent load admittance is $Y_L = G_L - jB_L$ *where:*

$$G_L = \frac{P_L}{V^2}, \qquad B_L = \frac{Q_L}{V^2} \qquad 2.11$$

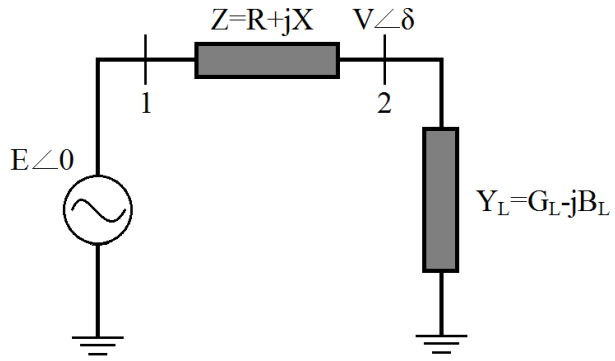

Figure 2.4 Single line diagram of a two-bus system to explain the P-index

If the load at node 2 increased by the amounts ΔP and ΔQ while maintaining a constant power factor, the corresponding load admittance increases by the amounts ΔG_L and ΔB_L. This increase in loading will cause a voltage change by an amount of ΔV which is typically negative (voltage drop). The new voltage at the load bus becomes $V + \Delta V$. The change in power at that particular bus becomes:

$$\begin{aligned} \Delta P_L &= (V + \Delta V)^2 (G_L + \Delta G_L) - V^2 G_L \\ &= (V + \Delta V)^2 \Delta G_L + (2V + \Delta V) G_L \Delta V \end{aligned} \qquad 2.12$$

The first term, $(V + \Delta V)^2 \Delta G_L$, which is positive, represents the increase in power due to the connection of extra load (ΔG_L) to the bus. The second term, $(2V + \Delta V) G_L \Delta V$, which is negative, represents the power lost on the original load (G_L) due to the drop in voltage (ΔV). The net power at the bus is the sum of these two opposing terms. At the voltage stability limit or voltage collapse point, these two terms cancel each other and the change in power (ΔP) becomes 0.

The P-index is defined as the ratio between these two opposing terms:

$$P_{index} = -\frac{(2V + \Delta V) G_L}{(V + \Delta V)^2} \cdot \frac{\Delta V}{\Delta G_L} \qquad 2.13$$

The negative sign was introduced in the previous equation to provide a positive index when there is a negative voltage drop (ΔV) for a positive change in load (ΔG_L).

In the limiting case as $\Delta G_L,\ \Delta V\ \rightarrow 0$, the P-index equation becomes:

$$P_{index} = -\frac{2G_L}{V} \cdot \frac{dV}{dG_L} \qquad 2.14$$

The term $\frac{dV}{dG_L}$ can be replaced by the more common term in network terminology $\frac{dV}{dP_L}$ as follows:

$$\frac{dV}{dG_L} = \frac{dV}{dP_L} \cdot \frac{dP_L}{dG_L} \qquad 2.15$$

From 2.11 it can be stated that:

$$dP_L = V^2 dG_L + 2VG_L dV \qquad 2.16$$

And:

$$\frac{dP_L}{dG_L} = V^2 + 2VG_L \frac{dV}{dG_L} \qquad 2.17$$

Substituting in 2.15:

$$\frac{dV}{dG_L} = \frac{dV}{dP_L}\left(V^2 + 2VG_L \frac{dV}{dG_L}\right) \qquad 2.18$$

Equation 2.18 can be expressed in a different format:

$$\frac{dV}{dG_L} = \frac{V^2 \frac{dV}{dP_L}}{1 - 2VG_L \frac{dV}{dP_L}} \qquad 2.19$$

Substituting 2.18 in the P-index formula (equation 2.14):

$$P_{index} = \frac{-2VG_L \frac{dV}{dP_L}}{1 - 2VG_L \frac{dV}{dP_L}} \quad 2.20$$

Using 2.11, P-index formula can be expressed in terms of active power as follows:

$$P_{index} = \frac{-2\frac{P_L}{V}\frac{dV}{dP_L}}{1 - 2\frac{P_L}{V}\frac{dV}{dP_L}} \quad 2.21$$

The P-index is a normalized index, and its value ranges between 0 (no load conditions of the system) and 1 (voltage collapse point). This characteristic makes it simpler to monitor the voltage stability and to identify critical nodes of the system.

2.5 Direct Computation of the Voltage Collapse Point

Another line of research uses direct methods to determine the voltage collapse point. This is done by formulating a set of non-linear equations that describe the system conditions at the point of collapse. Direct methods try to solve this set of equations. A recent method that uses the concept of Dog-Leg Trust Region Optimization is described in [22]. The following discussion explains how Dog-Leg Trust Region optimization combines the merits of conventional Line Search optimization methods and gets rid of their limitations.

For a certain objective function $f(x)$, Line Search methods define each new iteration as:

$$x_{k+1} = x_k + \Delta x_k \; = \; x_k + \sigma_k p_k \quad 2.22$$

Where σ_k is the Step length and p_k is the step direction.

These Line Search strategies can be subdivided into two methods. The first is the Steepest Descent technique where p_k is defined as:

$$p_k = -\nabla f(x_k)/\|\nabla f(x_k)\| \qquad 2.23$$

This direction guarantees a monotone decrease in $f(x)$. However, the method faces computational difficulties when determining the step length.

The other line search technique is the Newton Direction where $f(x)$ is approximated around x_k using the second-order Taylor expansion. The approximation is referred to as the model function and Δx_k is calculated as:

$$\Delta x_k = -H(x_k)^{-1}\nabla f(x_k) \qquad 2.24$$

Where $H(x_k)$ is the second derivative (Hessian) of the objective function.

This method is fast but might face convergence issues when the objective function and the model function are not very similar.

Similar to the Newton Search, Trust Region methods simplify the problem by using a quadratic model function. The technique first defines a neighborhood around x_k which is referred to as the trust region. The algorithm then searches for the minimizer of the model function inside that region. Most practical schemes start with an initial trust radius and update it based on the performance of the algorithm.

In the Dog-Leg scheme, a trajectory is defined by the two line segments joining x_k , x_k^{CP} (Steepest Descent solution) and x_k^{NP} (Newton Solution) respectively as shown in Figure 2.5.

If x_k^{CP} lays at the boundary of the trust region, it is considered as a solution. However, If x_k^{NP} falls inside the trust region, it is considered as the solution. Otherwise, the point of intersection

x_k^{SEC} between the dog-leg trajectory and the boundaries of the trust region is taken as the next step.

It is worth noting that this method has succeeded in calculating the maximum loading point with a small negligible error.

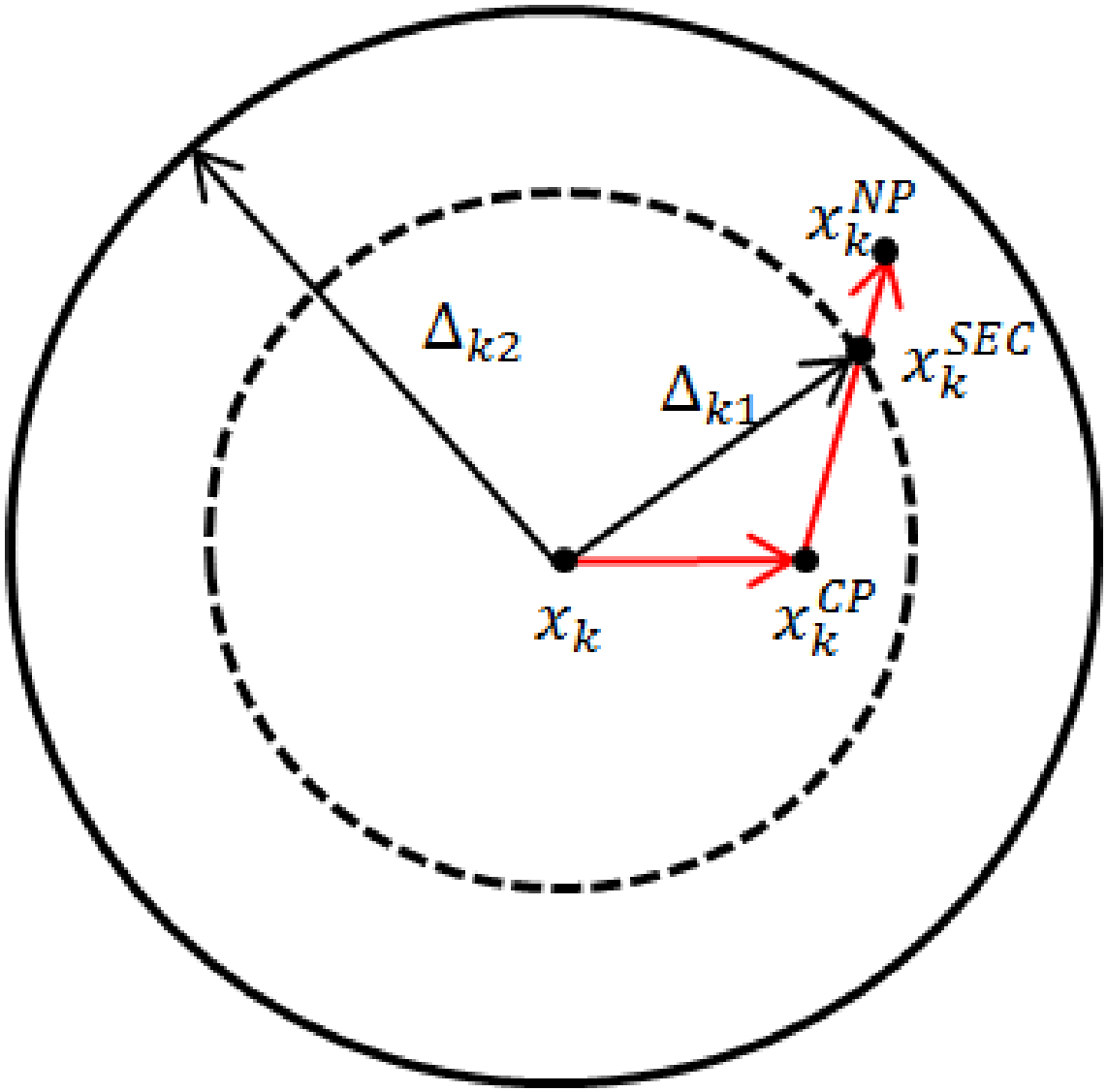

Figure 2.5 Trust-region optimization trajectories and boundaries

CHAPTER 3

METHODOLOGY

3.1 Distance to Voltage Collapse Using the P-index

As stated in [21], the P-index is able to calculate the distance to voltage collapse point if the term $\frac{dV}{dG_L}$ in equation 2.14 is assumed to be constant. Considering the two-bus system in Figure 2.4, the voltage at node 2 is calculated as follows:

$$\bar{V} = \bar{E} - \frac{\bar{E}}{\bar{Z}_L + \bar{Z}} \cdot \bar{Z} = \bar{E} - \frac{\bar{E}}{\frac{1}{\bar{Y}_L} + \bar{Z}} \cdot \bar{Z} \qquad 3.1$$

Where:

$\bar{Z} = \bar{R} + j\bar{X}$

$\bar{Y}_L = \bar{G}_L - j\bar{B}_L = \bar{G}_L(1 - j \cdot tan\phi)$

An approximation is made in [21] for small values of line impedance ($\bar{Z}$) and load admittance ($\bar{Y}_L$). Following this approximation, the voltage in 3.1 can be expressed as:

$$\bar{V} = \bar{E} - \bar{E}\bar{Z}\frac{1}{\bar{Z}_L} = \bar{E} - \bar{E}\bar{Z}\bar{Y}_L \qquad 3.2$$

Assuming a constant power factor and purely inductive line impedance. The voltage magnitude can be calculated as:

$$V = |E - jEXG_L(1 - jtan\phi)| = |E(1 - XG_L tan\phi) - jEXG_L| \qquad 3.3$$

The imaginary part in 3.3 is small compared to the real part. Hence, it can be neglected. The voltage magnitude then becomes:

$$V \approx E(1 - XG_L tan\phi) \qquad 3.4$$

Taking the derivative of 3.4 leads to:

$$\frac{dV}{dG_L} \approx -EXtan\phi \qquad 3.5$$

This approximation suggests a linear relationship between V and G_L. However, as shown in Figure 3.1, an analysis of the IEEE 14-bus system, the relationship between V and G_L is not perfectly linear. Rather, $\frac{dV}{dG_L}$ depends on G_L and its higher orders.

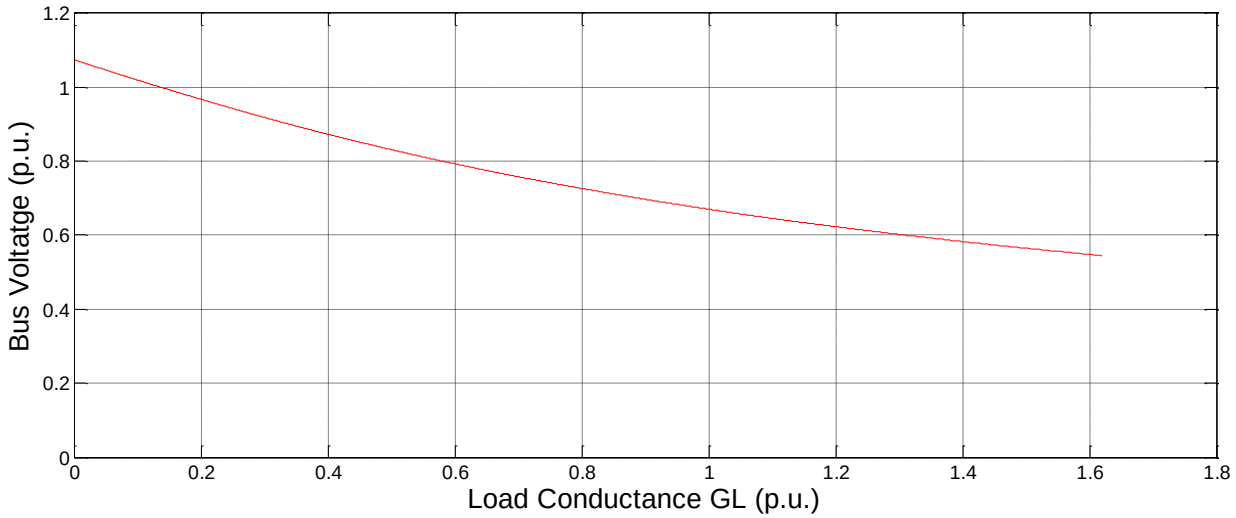

Figure 3.1 Actual V-GL relationship of bus 14 in The IEEE 14-bus system with line 13-14 outage

Unlike the previous analysis, this work does not approximate the relationship of the transmission line impedance ($\bar{Z}$) and load admittance ($\bar{Y}$) of the two-bus system. Continuing from (3.1), the voltage at node 2 then becomes:

$$\bar{V} = \bar{E}\left(1 - \frac{\bar{Z} \cdot \bar{Y}_L}{1 + \bar{Z} \cdot \bar{Y}_L}\right) = \bar{E} \cdot \frac{1}{1 + \bar{Z} \cdot \bar{Y}_L} \tag{3.6}$$

Substituting $\bar{Z} = j\bar{X}$ and $\bar{Y}_L = \bar{G}_L(1 - j \cdot tan\phi)$ results in:

$$\bar{V} = \bar{E} \cdot \frac{1}{1 + j\bar{X} \cdot \bar{G}_L(1 - j \cdot tan\phi)} \tag{3.7}$$

Grouping the real parts and imaginary parts of the denominator yields:

$$\bar{V} = \bar{E} \cdot \frac{1}{1 + \bar{X} \cdot \bar{G}_L \cdot tan\phi + j\bar{X} \cdot \bar{G}_L} \tag{3.8}$$

The voltage magnitude then becomes:

$$\begin{aligned} V &= \left| E \cdot \frac{1}{1 + jX \cdot G_L(1 - j \cdot tan\phi)} \right| \\ &= E \cdot \frac{1}{\sqrt{(1 + X \cdot G_L \cdot tan\phi)^2 + (X \cdot G_L)^2}} \end{aligned} \tag{3.9}$$

Further manipulation of equation 3.9 gives:

$$V = E \cdot \frac{1}{\sqrt{1 + 2X \cdot G_L \cdot tan\phi + X^2 \cdot G_L^2(1 + tan^2\phi)}} \tag{3.10}$$

V can be represented in terms of G_L as follows:

$$V = \frac{a}{\sqrt{1 + bG_L + cG_L^2}} \tag{3.11}$$

Where:

$a = E$

$$b = 2X \cdot tan\phi$$

$$c = X^2(1 + tan^2\phi)$$

The change in voltage for a change in load conductance $\frac{dV}{dG_L}$, which was considered linear in previous work, can be calculated by taking the derivative of equation 3.11 with respect to G_L. This results in the following:

$$\frac{dV}{dG_L} = \frac{-a(b + 2cG_L)}{2(1 + bG_L + cG_L^2)\sqrt{1 + bG_L + cG_L^2}} = \frac{-a(b + 2cG_L)}{2(1 + bG_L + cG_L^2)^{\frac{3}{2}}} \quad 3.12$$

From equation 3.12, $\frac{dV}{dG_L}$ is now dependent on G_L and its higher orders. Figure 3.2 shows the voltage and load conductance relationship for bus 14 in the IEEE 14-bus system with an outage of line 13-14. A comparison between the actual V-GL relationship, the proposed method V-GL relationship, which was plotted using equation 3.12, and the linear method relationship is presented in that figure. The V-GL plot of the actual relationship and the proposed method are almost identical.

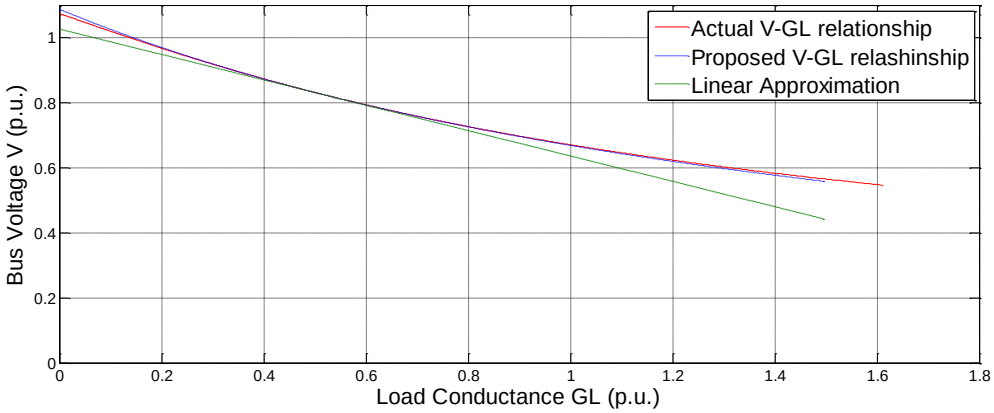

Figure 3.2 Comparison of V-GL relationship between linear method and the new models

Equation 3.11, along with the P-index equation 2.14, can be used to calculate voltage and load conductance at the point of collapse (V_m and G_{Lm}). As discussed earlier, the P-index = 1 at the point of collapse. Then:

$$\frac{dV}{dG_L} = \frac{-a(b + 2cG_{Lm})}{2(1 + bG_{Lm} + cG_{Lm}^2)^{\frac{3}{2}}} = -\frac{V_m}{2G_{Lm}} \tag{3.13}$$

Substituting V from 3.11 into 3.13 gives

$$\frac{-a(b + 2cG_{Lm})}{2\sqrt{1 + bG_{Lm} + cG_{Lm}^2}(1 + bG_{Lm} + cG_{Lm}^2)} = \frac{-a}{2G_{Lm}\sqrt{1 + bG_{Lm} + cG_{Lm}^2}} \tag{3.14}$$

Solving 3.14 for G_{Lm}:

$$G_{Lm} = \frac{1}{\sqrt{c}} \tag{3.15}$$

The next step is to find the voltage at the maximum loading point by substituting equation 3.15 in equation 3.11. Then, the active power loading at that point can be calculated using equation 2.11:

$$P_m = V_m^2 G_{Lm} \tag{3.16}$$

Or, in terms of loading multiplier λ_m:

$$\lambda_m = \frac{V_m^2 G_{Lm}}{P_0} \tag{3.17}$$

3.1.1 Calculating the Constants a, b, and c

When the P-index value of the most critical node of the system reaches 0.5, an alarm is raised to indicate voltage instability. This value was proposed in [21] and deemed worthy as an indicator. The values of the constants a, b, and c can be computed from that point in two different approaches that are explained in the following subsections.

3.1.1.1 The Simplified Approach

In this approach, an approximation is made for the coefficient $'a'$, where it is set as the voltage at no-load condition. This voltage is calculated by letting $I_L = 0$ in the following system admittance equation:

$$\begin{bmatrix} -I_L \\ I_G \end{bmatrix} = [Y] \begin{bmatrix} V_L \\ V_G \end{bmatrix} = \begin{bmatrix} Y_{LL} & Y_{LG} \\ Y_{GL} & Y_{GG} \end{bmatrix} \begin{bmatrix} V_L \\ V_G \end{bmatrix} \quad 3.18$$

Solving 3.18 for V_{L0}:

$$a = V_{L0} = -Y_{LL}^{-1} * Y_{LG} * V_G \quad 3.19$$

This leaves us with two unknowns, b and c. Two system equations are required to find these unknowns. The first equation is 3.12 where $\frac{dV}{dG_L}$ is calculated at P-index = 0.5:

$$\left.\frac{dV}{dG_L}\right|_{0.5} = \frac{-a(b + 2cG_{L0.5})}{2(1 + bG_{L0.5} + cG_{L0.5}^2)^{\frac{3}{2}}} \quad 3.20$$

The second system equation is obtained by substituting the voltage (V) and load conductance (G_L) acquired at P-index = 0.5, as well as $a = V_0$ in equation 3.11:

$$V_{0.5} = \frac{a}{\sqrt{1 + bG_{L0.5} + cG_{L0.5}^2}} \quad 3.21$$

Solving equations 3.20 and 3.21 to find b and c yield:

$$b = \frac{2a^2}{V_{0.5}^3}\frac{dV}{dG_L}\Big|_{0.5} - \frac{2(V_{0.5}^2 - a^2)}{G_{L0.5}^2 V_{0.5}^3} \quad 3.22$$

And:

$$c = \frac{V_{0.5}^3 - V_{0.5}a^2 - G_{L0.5}a^2\frac{dV}{dG_L}\Big|_{0.5}}{G_{L0.5}^2 V_{0.5}^3} \quad 3.23$$

3.1.1.2 The Second Derivative Approach

In this approach, all the constants (a, b, and c) are computed from the system conditions when the P-index = 0.5. A set of three system equations are required to find the three unknowns. Two equations were already established in the first approach (3.20 and 3.21). The third equation can be obtained by taking the derivative of $\frac{dV}{dG_L}$ in equation 3.12. This results in:

$$\frac{d^2V}{dG_L^2} = \frac{3a(b + 2cG_{L0.5})^2}{4(1 + bG_{L0.5} + cG_{L0.5}^2)^{\frac{5}{2}}} - \frac{ac}{(1 + bG_{L0.5} + cG_{L0.5}^2)^{\frac{3}{2}}} \quad 3.24$$

Solving equations 3.20, 3.21 and 3.24 to find a, b and c gives:

$$a = \frac{V_{0.5}^2}{\sqrt{V_{0.5}^2 + 2V_{0.5}G_{L0.5}\frac{dV}{dG_L}\Big|_{0.5} + 3\left(G_{L0.5}\frac{dV}{dG_L}\Big|_{0.5}\right)^2 - V_{0.5}G_{L0.5}^2\frac{d^2V}{dG_L^2}\Big|_{0.5}}} \quad 3.25$$

$$b = \frac{2V_{0.5}G_{L0.5}\left.\frac{d^2V}{dG_L^2}\right|_{0.5} - 6G_{L0.5}\left(\left.\frac{dV}{dG_L}\right|_{0.5}\right)^2 - 2V_{0.5}\left.\frac{dV}{dG_L}\right|_{0.5}}{V_{0.5}^2 + 2V_{0.5}G_{L0.5}\left.\frac{dV}{dG_L}\right|_{0.5} + 3\left(G_{L0.5}\left.\frac{dV}{dG_L}\right|_{0.5}\right)^2 - V_{0.5}G_{L0.5}^2\left.\frac{d^2V}{dG_L^2}\right|_{0.5}} \quad 3.26$$

And:

$$c = \frac{3\left(\left.\frac{dV}{dG_L}\right|_{0.5}\right)^2 - V\frac{d^2V}{dG_L^2}}{V_{0.5}^2 + 2V_{0.5}G_{L0.5}\left.\frac{dV}{dG_L}\right|_{0.5} + 3\left(G_{L0.5}\left.\frac{dV}{dG_L}\right|_{0.5}\right)^2 - V_{0.5}G_{L0.5}^2\left.\frac{d^2V}{dG_L^2}\right|_{0.5}} \quad 3.27$$

3.1.2 Calculating the Second Derivative

The new term in the previous equations $\left(\frac{d^2V}{dG_L^2}\right)$ can be calculated from the system conditions at P-index = 0.5. Substituting the term $\frac{dP_L}{dG_L}$ from equation 2.17 in 2.15 gives:

$$\frac{dV}{dG_L} = \frac{dV}{dP_L}\left(V^2 + 2VG_L\frac{dV}{dG_L}\right) \quad 3.28$$

Taking the derivative with respect to G_L:

$$\frac{d^2V}{dG_L^2} = \frac{dV}{dP_L}\left(2V\frac{dV}{dG_L} + 2VG_L\frac{d^2V}{dG_L^2} + 2G_L\left(\frac{dV}{dG_L}\right)^2 + 2V\frac{dV}{dG_L}\right) + \frac{d^2V}{dP_L^2}\cdot\frac{dP_L}{dG_L}\left(V^2 + 2VG_L\frac{dV}{dG_L}\right) \quad 3.29$$

Collecting the terms:

$$\frac{d^2V}{dG_L^2} = \frac{dV}{dP_L}\left(4V\frac{dV}{dG_L} + 2VG_L\frac{d^2V}{dG_L^2} + 2G_L\left(\frac{dV}{dG_L}\right)^2\right) + \frac{d^2V}{dP_L^2}.\frac{dP_L}{dG_L}\left(V^2 + 2VG_L\frac{dV}{dG_L}\right)^2 \quad 3.30$$

Substituting the term $\frac{dP_L}{dG_L}$, from equation 2.17 again gives:

$$\frac{d^2V}{dG_L^2}\left(1 - 2VG_L\frac{dV}{dP_L}\right) = \frac{dV}{dP_L}\left(4V\frac{dV}{dG_L} + 2G_L\left(\frac{dV}{dG_L}\right)^2\right) + \frac{d^2V}{dP_L^2}\left(V^2 + 2VG_L\frac{dV}{dG_L}\right)^2 \quad 3.31$$

With further manipulation:

$$\frac{d^2V}{dG_L^2} = \frac{\frac{dV}{dP_L}\left(4V\frac{dV}{dG_L} + 2G_L\left(\frac{dV}{dG_L}\right)^2\right) + \frac{d^2V}{dP_L^2}\left(V^2 + 2VG_L\frac{dV}{dG_L}\right)^2}{\left(1 - 2VG_L\frac{dV}{dP_L}\right)} \quad 3.32$$

All the terms in equation 3.32 are immediately available except for $\frac{d^2V}{dP_L^2}$. This term needs to be calculated from the system power flow equations. Consider the following power flow equation:

$$\begin{bmatrix} \Delta P_1 \\ \vdots \\ \Delta P_i \\ \vdots \\ \Delta Q_1 \\ \vdots \\ \Delta Q_i \\ \vdots \end{bmatrix} = \begin{bmatrix} \frac{\partial P_1}{\partial \delta_1} & \cdots & \frac{\partial P_1}{\partial \delta_i} & \cdots & \frac{\partial P_1}{\partial V_1} & \cdots & \frac{\partial P_1}{\partial V_i} & \cdots \\ \vdots & \ddots & \vdots & \ddots & \vdots & \ddots & \vdots & \ddots \\ \frac{\partial P_i}{\partial \delta_1} & \cdots & \frac{\partial P_i}{\partial \delta_i} & \cdots & \frac{\partial P_i}{\partial V_1} & \cdots & \frac{\partial P_i}{\partial V_i} & \cdots \\ \vdots & \ddots & \vdots & \ddots & \vdots & \ddots & \vdots & \ddots \\ \frac{\partial Q_1}{\partial \delta_1} & \cdots & \frac{\partial Q_1}{\partial \delta_i} & \cdots & \frac{\partial Q_1}{\partial V_1} & \cdots & \frac{\partial Q_1}{\partial V_i} & \cdots \\ \vdots & \ddots & \vdots & \ddots & \vdots & \ddots & \vdots & \ddots \\ \frac{\partial Q_i}{\partial \delta_1} & \cdots & \frac{\partial Q_i}{\partial \delta_i} & \cdots & \frac{\partial Q_i}{\partial V_1} & \cdots & \frac{\partial Q_i}{\partial V_i} & \cdots \\ \vdots & \ddots & \vdots & \ddots & \vdots & \ddots & \vdots & \ddots \end{bmatrix} \cdot \begin{bmatrix} \Delta\delta_1 \\ \vdots \\ \Delta\delta_i \\ \vdots \\ \Delta V_1 \\ \vdots \\ \Delta V_i \\ \vdots \end{bmatrix} \quad 3.33$$

Or, in short:

$$\begin{bmatrix}\Delta P\\ \Delta Q\end{bmatrix} = [J].\begin{bmatrix}\Delta\delta\\ \Delta V\end{bmatrix} \quad 3.34$$

The Jacobian Matrix J can be represented as four submatrices:

$$J = \begin{bmatrix}\frac{\partial P_i}{\partial \delta_k} & \frac{\partial P_i}{\partial V_k}\\ \frac{\partial Q_i}{\partial \delta_k} & \frac{\partial Q_i}{\partial V_k}\end{bmatrix} = \begin{bmatrix}J_{11} & J_{12}\\ J_{21} & J_{22}\end{bmatrix} \quad 3.35$$

Dividing by ΔP_i:

$$\begin{bmatrix}\alpha_{1i}\\ \vdots\\ 1\\ \vdots\\ \beta_1\alpha_{1i}\\ \vdots\\ \beta_i\\ \vdots\end{bmatrix} = \begin{bmatrix}\frac{\partial P_1}{\partial \delta_1} & \cdots & \frac{\partial P_1}{\partial \delta_i} & \cdots & \frac{\partial P_1}{\partial V_1} & \cdots & \frac{\partial P_1}{\partial V_i} & \cdots\\ \vdots & \ddots & \vdots & \ddots & \vdots & \ddots & \vdots & \ddots\\ \frac{\partial P_i}{\partial \delta_1} & \cdots & \frac{\partial P_i}{\partial \delta_i} & \cdots & \frac{\partial P_i}{\partial V_1} & \cdots & \frac{\partial P_i}{\partial V_i} & \cdots\\ \vdots & \ddots & \vdots & \ddots & \vdots & \ddots & \vdots & \ddots\\ \frac{\partial Q_1}{\partial \delta_1} & \cdots & \frac{\partial Q_1}{\partial \delta_i} & \cdots & \frac{\partial Q_1}{\partial V_1} & \cdots & \frac{\partial Q_1}{\partial V_i} & \cdots\\ \vdots & \ddots & \vdots & \ddots & \vdots & \ddots & \vdots & \ddots\\ \frac{\partial Q_i}{\partial \delta_1} & \cdots & \frac{\partial Q_i}{\partial \delta_i} & \cdots & \frac{\partial Q_i}{\partial V_1} & \cdots & \frac{\partial Q_i}{\partial V_i} & \cdots\\ \vdots & \ddots & \vdots & \ddots & \vdots & \ddots & \vdots & \ddots\end{bmatrix}.\begin{bmatrix}\frac{\mathrm{d}\delta_1}{dP_i}\\ \vdots\\ \frac{\mathrm{d}\delta_i}{dP_i}\\ \vdots\\ \frac{\mathrm{d}V_1}{dP_i}\\ \vdots\\ \frac{\mathrm{d}V_i}{dP_i}\\ \vdots\end{bmatrix} \quad 3.36$$

Where:

$$\alpha_{ki} = \frac{\Delta P_k}{\Delta P_i}$$

$$\beta_k = \frac{\Delta Q_k}{\Delta P_k}$$

Taking derivatives with respect to P_i:

$$\begin{bmatrix}0\\ \vdots\\ 0\\ \vdots\\ 0\\ \vdots\end{bmatrix}=\begin{bmatrix}\frac{d}{dP_i}\left(\frac{\partial P_1}{\partial \delta_1}\right) & \cdots & \frac{d}{dP_i}\left(\frac{\partial P_1}{\partial \delta_i}\right) & \cdots & \frac{d}{dP_i}\left(\frac{\partial P_1}{\partial V_1}\right) & \cdots & \frac{d}{dP_i}\left(\frac{\partial P_1}{\partial V_i}\right) & \cdots\\ \vdots & \ddots & \vdots & \ddots & \vdots & \ddots & \vdots & \ddots\\ \frac{d}{dP_i}\left(\frac{\partial P_i}{\partial \delta_1}\right) & \cdots & \frac{d}{dP_i}\left(\frac{\partial P_i}{\partial \delta_i}\right) & \cdots & \frac{d}{dP_i}\left(\frac{\partial P_i}{\partial V_1}\right) & \cdots & \frac{d}{dP_i}\left(\frac{\partial P_i}{\partial V_i}\right) & \cdots\\ \vdots & \ddots & \vdots & \ddots & \vdots & \ddots & \vdots & \ddots\\ \frac{d}{dP_i}\left(\frac{\partial Q_1}{\partial \delta_1}\right) & \cdots & \frac{d}{dP_i}\left(\frac{\partial Q_1}{\partial \delta_i}\right) & \cdots & \frac{d}{dP_i}\left(\frac{\partial Q_1}{\partial V_1}\right) & \cdots & \frac{d}{dP_i}\left(\frac{\partial Q_1}{\partial V_i}\right) & \cdots\\ \vdots & \ddots & \vdots & \ddots & \vdots & \ddots & \vdots & \ddots\\ \frac{d}{dP_i}\left(\frac{\partial Q_i}{\partial \delta_1}\right) & \cdots & \frac{d}{dP_i}\left(\frac{\partial Q_i}{\partial \delta_i}\right) & \cdots & \frac{d}{dP_i}\left(\frac{\partial Q_i}{\partial V_1}\right) & \cdots & \frac{d}{dP_i}\left(\frac{\partial Q_i}{\partial V_i}\right) & \cdots\\ \vdots & \ddots & \vdots & \ddots & \vdots & \ddots & \vdots & \ddots\end{bmatrix}.\begin{bmatrix}\frac{\mathrm{d}\delta_1}{dP_i}\\ \vdots\\ \frac{\mathrm{d}\delta_i}{dP_i}\\ \vdots\\ \frac{\mathrm{d}V_1}{dP_i}\\ \vdots\\ \frac{\mathrm{d}V_i}{dP_i}\\ \vdots\end{bmatrix}+$$

$$\begin{bmatrix}\frac{\partial P_1}{\partial \delta_1} & \cdots & \frac{\partial P_1}{\partial \delta_i} & \cdots & \frac{\partial P_1}{\partial V_1} & \cdots & \frac{\partial P_1}{\partial V_i} & \cdots\\ \vdots & \ddots & \vdots & \ddots & \vdots & \ddots & \vdots & \ddots\\ \frac{\partial P_i}{\partial \delta_1} & \cdots & \frac{\partial P_i}{\partial \delta_i} & \cdots & \frac{\partial P_i}{\partial V_1} & \cdots & \frac{\partial P_i}{\partial V_i} & \cdots\\ \vdots & \ddots & \vdots & \ddots & \vdots & \ddots & \vdots & \ddots\\ \frac{\partial Q_1}{\partial \delta_1} & \cdots & \frac{\partial Q_1}{\partial \delta_i} & \cdots & \frac{\partial Q_1}{\partial V_1} & \cdots & \frac{\partial Q_1}{\partial V_i} & \cdots\\ \vdots & \ddots & \vdots & \ddots & \vdots & \ddots & \vdots & \ddots\\ \frac{\partial Q_i}{\partial \delta_1} & \cdots & \frac{\partial Q_i}{\partial \delta_i} & \cdots & \frac{\partial Q_i}{\partial V_1} & \cdots & \frac{\partial Q_i}{\partial V_i} & \cdots\\ \vdots & \ddots & \vdots & \ddots & \vdots & \ddots & \vdots & \ddots\end{bmatrix}.\begin{bmatrix}\frac{\partial^2 \delta_1}{\partial P_i^2}\\ \vdots\\ \frac{\partial^2 \delta_i}{\partial P_i^2}\\ \vdots\\ \frac{\partial^2 V_1}{\partial P_i^2}\\ \vdots\\ \frac{\partial^2 V_i}{\partial P_i^2}\\ \vdots\end{bmatrix} \qquad 3.37$$

Or, in short:

$$\begin{bmatrix}0\\ 0\end{bmatrix}=[H].\begin{bmatrix}\frac{\mathrm{d}\delta}{dP_i}\\ \frac{\mathrm{d}V}{dP_i}\end{bmatrix}+[J].\begin{bmatrix}\frac{\partial^2 \delta}{dP_i^2}\\ \frac{\partial^2 V}{dP_i^2}\end{bmatrix} \qquad 3.38$$

Where H is the Hessian matrix.

$$H = \begin{bmatrix} \frac{d}{dP_i}\left(\frac{\partial P_1}{\partial \delta_1}\right) & \cdots & \frac{d}{dP_i}\left(\frac{\partial P_1}{\partial \delta_i}\right) & \cdots & \frac{d}{dP_i}\left(\frac{\partial P_1}{\partial V_1}\right) & \cdots & \frac{d}{dP_i}\left(\frac{\partial P_1}{\partial V_i}\right) & \cdots \\ \vdots & \ddots & \vdots & \ddots & \vdots & \ddots & \vdots & \ddots \\ \frac{d}{dP_i}\left(\frac{\partial P_i}{\partial \delta_1}\right) & \cdots & \frac{d}{dP_i}\left(\frac{\partial P_i}{\partial \delta_i}\right) & \cdots & \frac{d}{dP_i}\left(\frac{\partial P_i}{\partial V_1}\right) & \cdots & \frac{d}{dP_i}\left(\frac{\partial P_i}{\partial V_i}\right) & \cdots \\ \vdots & \ddots & \vdots & \ddots & \vdots & \ddots & \vdots & \ddots \\ \frac{d}{dP_i}\left(\frac{\partial Q_1}{\partial \delta_1}\right) & \cdots & \frac{d}{dP_i}\left(\frac{\partial Q_1}{\partial \delta_i}\right) & \cdots & \frac{d}{dP_i}\left(\frac{\partial Q_1}{\partial V_1}\right) & \cdots & \frac{d}{dP_i}\left(\frac{\partial Q_1}{\partial V_i}\right) & \cdots \\ \vdots & \ddots & \vdots & \ddots & \vdots & \ddots & \vdots & \ddots \\ \frac{d}{dP_i}\left(\frac{\partial Q_i}{\partial \delta_1}\right) & \cdots & \frac{d}{dP_i}\left(\frac{\partial Q_i}{\partial \delta_i}\right) & \cdots & \frac{d}{dP_i}\left(\frac{\partial Q_i}{\partial V_1}\right) & \cdots & \frac{d}{dP_i}\left(\frac{\partial Q_i}{\partial V_i}\right) & \cdots \\ \vdots & \ddots & \vdots & \ddots & \vdots & \ddots & \vdots & \ddots \end{bmatrix} \quad 3.39$$

Formulation of the Hessian matrix is carried out in the Appendix.

After forming the Hessian matrix (H), one can proceed to find the second derivative $\frac{d^2V}{dP_i^2}$. Equation 3.38 can be rewritten in the following format:

$$\begin{bmatrix} \frac{d^2\delta}{dP_i^2} \\ \frac{d^2V}{dP_i^2} \end{bmatrix} = -[J]^{-1}\left([H].\begin{bmatrix} \frac{\mathrm{d}\delta}{dP_i} \\ \frac{\mathrm{d}V}{dP_i} \end{bmatrix}\right) \quad 3.40$$

The second derivative obtained from equation 3.40 can now be used to calculate $\frac{d^2V}{dG_L^2}$ using equation 3.32. This value can be used in turn to calculate the constants a, b, and c.

3.2 Generators' Reactive Power Limits

When a generator reaches its reactive limits, it can no longer support the voltage and the generator bus is treated as a load bus from that point. Reactive Power limits affect the maximum loadability of the system. Hence, it must be considered when calculating the distance to collapse point.

In this work, the generators reactive power limit was accounted for successfully. The reactive power injection of all the generators was monitored as the loading increase until the point where the maximum P-index=0.5. When a generator reaches its reactive limit before or at that point, the corresponding bus is reset as a load bus and its reactive power increment ΔQ in the Jacobian matrix set to 0. The P-index is then recalculated again for all the load buses of the system as it will gain a larger increment.

In some cases, generators might reach their reactive power limit between the point of voltage stability limit prediction at P-index = 0.5 and the point of collapse itself. It becomes difficult to model the behavior of the reactive power between those two points. Further research is required to model the behavior of the system when subjected to reactive power limits.

CHAPTER 4

RESULTS AND DISCUSSION

4.1 Introduction

A MATLAB prototype of the new methods was written to predict the voltage collapse point for IEEE 14, 39, 57, 118, and 300-bus systems. Furthermore, selected outages were performed, and the methods were tested and compared for these outages.

4.2 Tests Without Generators' Reactive Limits

4.2.1 Testing the Methods on the IEEE 14-bus System

The new methods were tested on all possible outages of the IEEE-14 bus system shown in Figure 4.1. The load multiplier was increased in steps and the P-index was calculated for each bus in the system. The voltage collapse point was calculated when the most critical node of the system, which is the bus with highest P-index value, reached a value of 0.5. Table 4.1 summarizes the results obtained from the simulation.

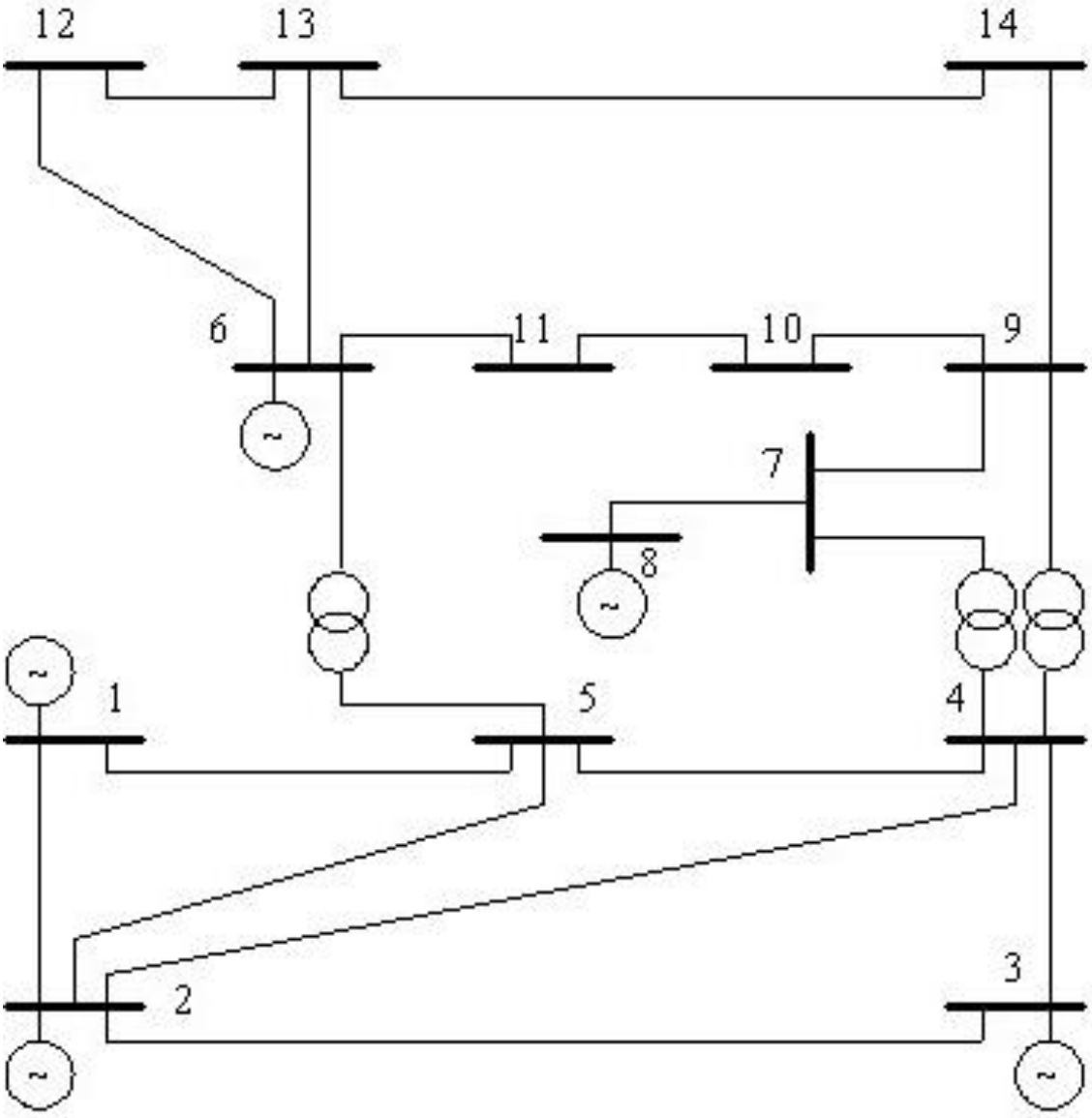

Figure 4.1 Single line diagram of the IEEE 14-bus system

Table 4.1 Comparison Between the New Methods and the Linear Method for the IEEE 14-bus System Without Considering Reactive Limits

Case	λ_m (Actual)	λ_m (Linear Method)	Error (%)	λ_m (Second Derivative Method)	Error (%)	λ_m ($a = V_0$ Method)	Error (%)
Intact	4.040	3.883	3.9	4.174	-3.3	4.214	-4.3
1-2 Out	1.343	1.489	-10.8	1.370	-2.0	1.438	-7.1
1-5 Out	3.658	3.583	2.0	3.645	0.3	3.656	0.06
2-3 Out	2.268	2.416	-6.5	2.318	-2.2	2.395	-5.6
2-4 Out	3.289	3.214	2.3	3.266	0.7	3.261	0.9
2-5 Out	3.429	3.327	3.0	3.396	1.0	3.383	1.3
3-4 Out	3.944	3.799	3.7	4.074	-3.3	4.122	-4.5
4-5 Out	3.940	3.742	5.0	4.113	-4.4	4.123	-4.6
4-7 Out	3.604	3.489	3.2	3.720	-3.2	3.772	-4.7
4-9 Out	3.942	3.731	5.4	4.058	-2.9	4.082	-3.6
5-6 Out	2.283	2.422	-6.1	2.341	-2.5	2.440	-6.9
6-11 Out	3.528	2.989	15.3	3.366	4.6	3.297	6.5
6-12 Out	3.981	3.718	6.6	4.059	-2.0	4.066	-2.1
6-13 Out	3.224	2.773	14.0	3.152	2.2	3.108	3.6
7-9 Out	2.876	2.554	11.2	2.827	1.7	2.794	2.9
9-10 Out	4.008	3.768	6.0	4.052	-1.1	4.070	-1.5
9-14 Out	3.702	3.248	12.3	3.690	0.3	3.679	0.6
10-11 Out	3.736	3.284	12.1	3.611	3.4	3.555	4.8
12-13 Out	4.029	3.825	5.1	4.136	-2.6	4.161	-3.3
13-14 Out	3.245	2.756	15.1	3.132	3.5	3.071	5.4
1-2 and 2-5	1.290	1.424	-10.4	1.271	1.5	1.323	-2.6
4-9 and 4-7	2.900	2.726	6.0	2.942	-1.4	2.960	-2.1
5-6 and 6-11	1.520	1.615	-6.3	1.549	-1.9	1.617	-6.4

The second derivative method provided the least error for the vast majority of the cases with a maximum error of 4.6% in the case of line 6-11 outage. By comparison, the linear method had an error of 15.3% and the $a = V_0$ approximation method's error was 7% for that particular outage. Table 4.2 provides the statistical analysis results for all three methods' performance.

Table 4.2 Statistical Analysis of Methods Performance for the IEEE 14-bus System Without Considering Reactive Limits

Method	Linear	Second Derivative	$a = V_0$
Mean Error	7.5	2.3	3.7
Standard Deviation	4.1	1.2	2.0
Max Error	15.3	4.6	7.7
Min Error	2.0	0.3	0.06

4.2.2 Testing the Methods on the IEEE 39-bus System

The two proposed methods were used to predict the voltage collapse point on different outages scenarios of the IEEE 39-bus system shown in Figure 4.2. Table 4.3 summarizes the results of these tests.

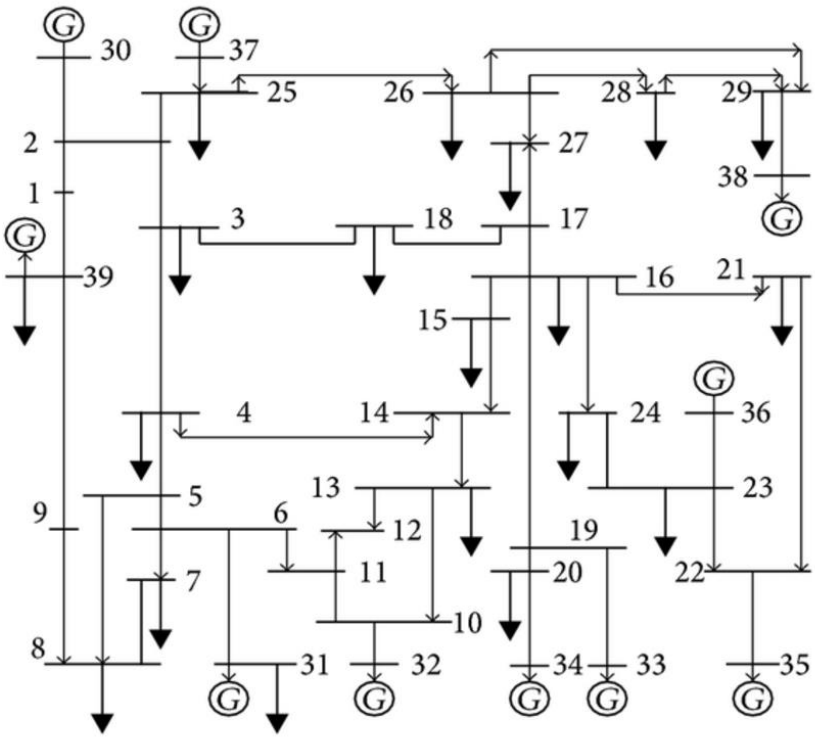

Figure 4.2 Single line diagram of the IEEE 39-bus system

Table 4.3 Comparison Between the New Methods and the Linear Method for the IEEE 39-bus System Without Considering Reactive Limits

Case	λ_m (Actual)	λ_m (Linear Method)	Error (%)	λ_m (Second Derivative Method)	Error (%)	λ_m ($a = V_0$ Method)	Error (%)
Intact	2.300	2.139	7.0	2.279	0.9	2.253	2.0
3-18 Out	2.295	2.115	7.8	2.261	1.5	2.231	2.8
6-7 Out	2.092	1.892	9.6	2.045	2.2	2.026	3.2
10-13 Out	2.199	1.981	9.9	2.145	2.5	2.117	3.7
15-16 Out	1.729	1.503	13.1	1.676	3.1	1.646	4.8
17-18 Out	2.260	2.097	7.2	2.238	1.0	2.207	2.3
17-27 Out	2.293	2.135	6.9	2.271	1.0	2.247	2.0
25-26 Out	2.255	2.094	7.1	2.233	1.0	2.204	2.3

The second derivative method provided the least error for all the tested cases in this system. The maximum error is 3.1% in case of line 15-16 outage. By comparison, the linear method had an error of 13.1% and the $a = V_0$ approximation method's error was 4.8% for that outage. Table 4.2 provides a statistical analysis of all three methods performance for this system.

Table 4.4 Statistical Analysis of Methods Performance for the IEEE 39-bus System Without Considering Reactive Limits

Method	Linear	Second Derivative	$a = V_0$
Mean Error	8.6	1.6	2.9
Standard Deviation	2.0	0.8	0.9
Max Error	13.1	3.1	4.8
Min Error	6.9	0.9	2.0

4.2.3 Testing the Methods on the IEEE 57-bus System

The two proposed methods were used to predict the voltage collapse point on selected outages scenarios on the IEEE 57-bus system shown in Figure 4.3. Table 4.5 summarizes the results of these tests.

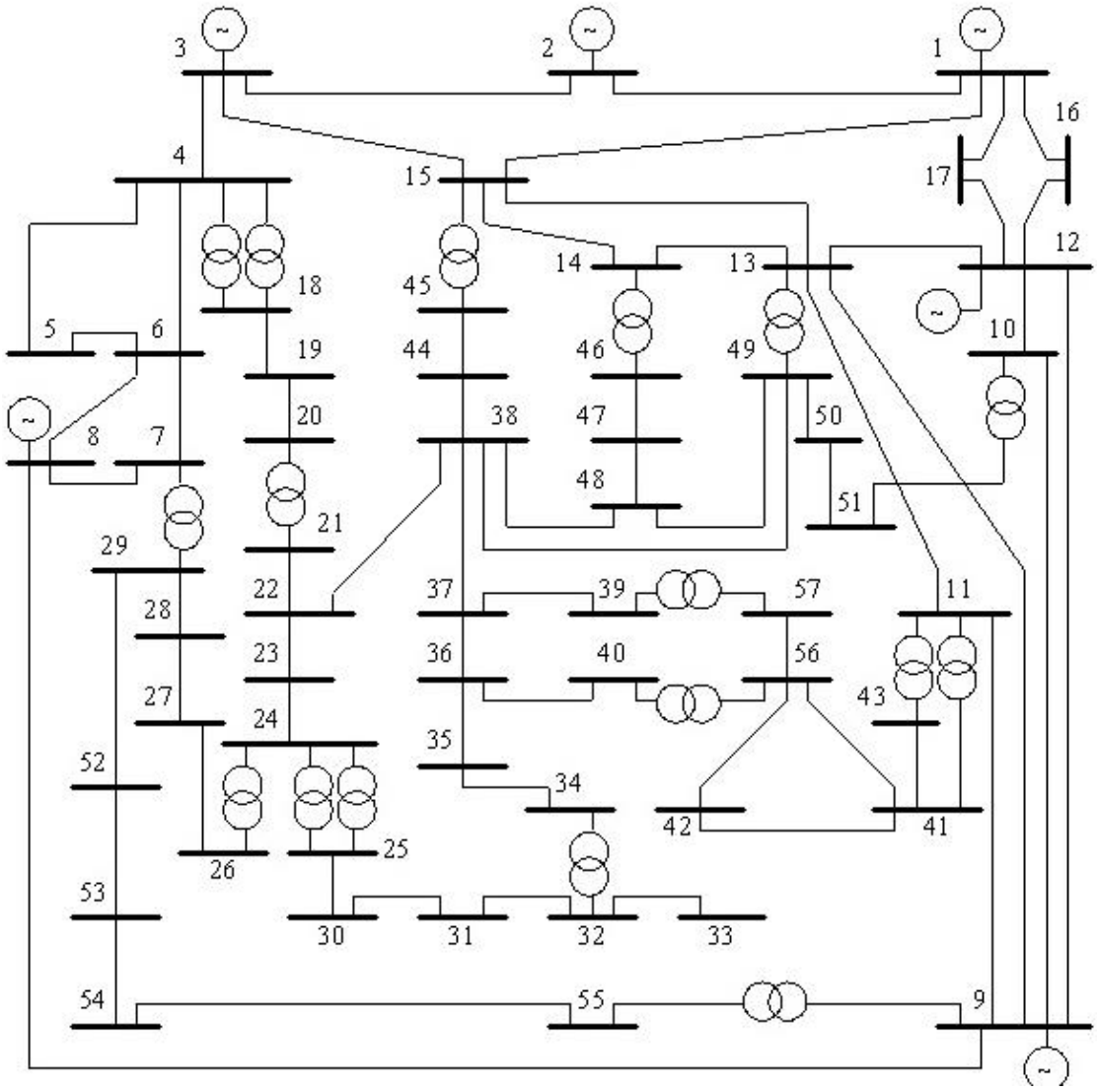

Figure 4.3 Single line diagram of the IEEE 57-bus system

Table 4.5 Comparison Between the New Methods and the Linear Method for the IEEE 57-bus System Without Considering Reactive Limits

Case	λ_m (Actual)	λ_m (Linear Method)	Error (%)	λ_m (Second Derivative Method)	Error (%)	λ_m ($a = V_0$ Method)	Error (%)
Intact	2.070	1.704	17.7	1.981	4.3	1.938	6.4
1-15 Out	2.020	1.664	17.6	1.941	3.9	1.902	5.8
7-29 Out	1.227	1.092	11.0	1.211	1.3	1.199	2.3
13-14 Out	2.030	1.675	17.5	1.948	4.0	1.905	6.2
22-38 Out	1.880	1.562	16.9	1.812	3.6	1.776	5.5
23-24 Out	1.940	1.620	16.5	1.871	3.6	1.835	5.4
24-26 Out	1.843	1.521	17.5	1.774	3.7	1.737	5.8
37-38 Out	1.243	1.090	12.3	1.217	2.1	1.201	3.4

The second derivative method provided the least error for all the tested cases in this system. The maximum error is 4.3% in case of intact system. by comparison, the linear method had an error of 17.7% and the $a = V_0$ approximation method's error was 6.4% for that case. Table 4.6 provides a statistical analysis of all three methods performance for this system.

Table 4.6 Statistical Analysis of Methods Performance for the IEEE 57-bus System Without Considering Reactive Limits

Method	Linear	Second Derivative	$a = V_0$
Mean Error	15.9	3.3	5.1
Standard Deviation	2.5	1.0	1.4
Max Error	17.7	4.3	6.4
Min Error	11.0	1.3	2.3

4.2.4 Testing the Methods on the IEEE 118-bus System

The two proposed methods were used to predict the voltage collapse point on different outages on the IEEE 118-bus system shown in Figure 4.4. Table 4.7 summarizes the results of these tests.

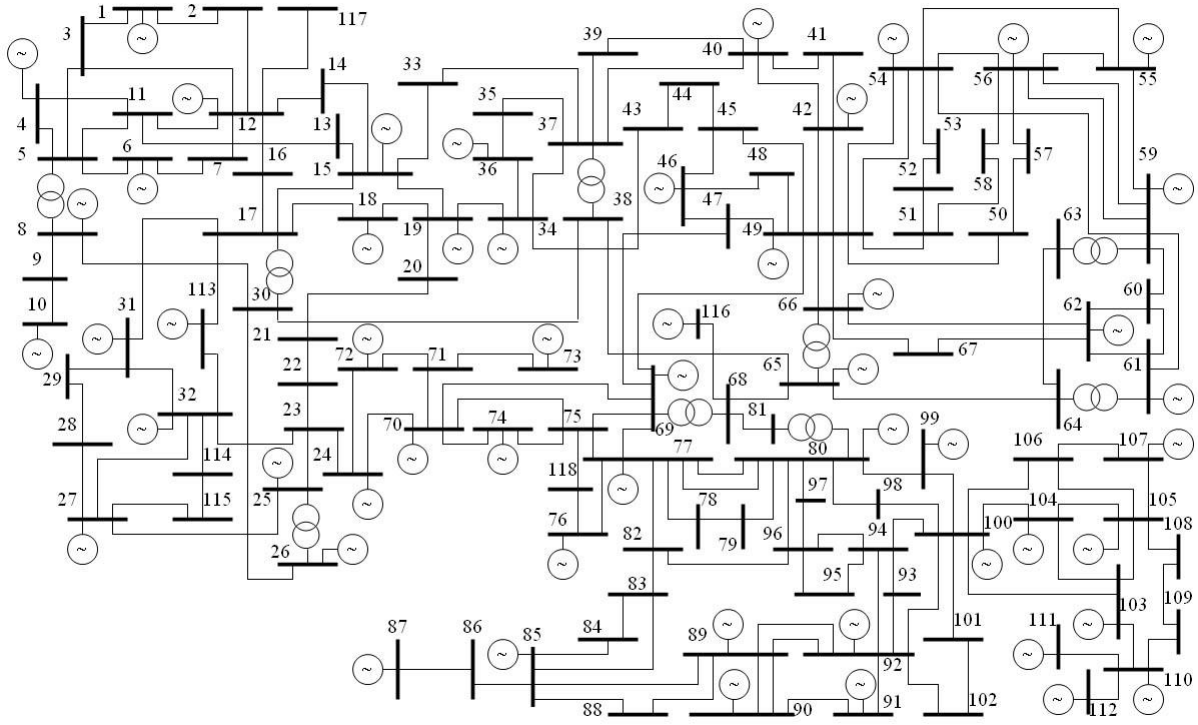

Figure 4.4 Single line diagram of the IEEE 118-bus system

Table 4.7 Comparison Between the New Methods and the Linear Method for the IEEE 118-bus System Without Considering Reactive Limits

Case	λ_m (Actual)	λ_m (Linear Method)	Error (%)	λ_m (Second Derivative Method)	Error (%)	λ_m ($a = V_0$ Method)	Error (%)
Intact	3.200	3.244	-1.4	3.262	-1.9	3.334	-4.2
26-30 Out	2.610	2.410	7.7	2.615	-0.2	2.499	4.3
49-69 Out	3.190	3.295	-3.3	3.277	-2.7	3.382	-6.0
23-24 Out	2.980	3.084	-3.5	3.052	-2.4	3.145	-5.5
68-69 Out	2.760	2.966	-7.5	2.782	-0.8	2.889	-4.7

The second derivative method provided the least error for the vast majority of the tested cases in this system. The maximum error is 2.7% in the case of line 49-69 outage. By comparison, the linear method had an error of 3.3% and $a = V_0$ approximation method's error was 6% for that case. Table 4.8 provides a statistical analysis of all three methods performance for this system.

Table 4.8 Statistical Analysis of Methods Performance for the IEEE 118-bus System Without Considering Reactive Limits

Method	Linear	Second Derivative	$a = V_0$
Mean Error	4.7	1.6	4.9
Standard Deviation	2.5	1.0	0.7
Max Error	7.7	2.7	6.0
Min Error	1.4	0.2	4.2

4.2.5 Testing the Methods on the IEEE 300-bus System

The two proposed methods were used to predict the voltage collapse point on different outages on the IEEE 300-bus system shown in Figure 4.5. Table 4.9 summarizes the results of these tests.

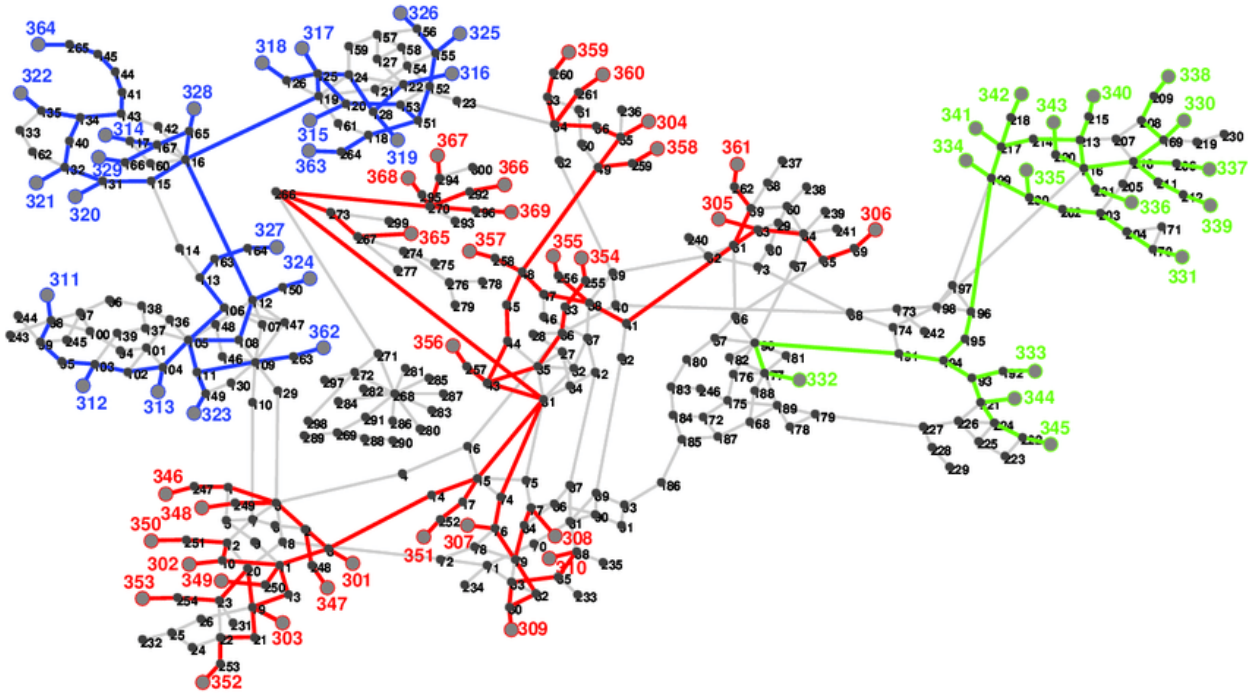

Figure 4.5 Single line diagram of the IEEE 300-bus system

Table 4.9 Comparison Between the New Methods and the Linear Method for the IEEE 300-bus System Without Considering Reactive Limits

Case	λ_m (Actual)	λ_m (Linear Method)	Error (%)	λ_m (Second Derivative Method)	Error (%)	λ_m ($a = V_0$ Method)	Error (%)
Intact	1.430	1.340	6.3	1.445	-1.0	1.410	1.4
3-4 Out	1.430	1.273	11.0	1.367	4.4	1.339	6.4
40-68 Out	1.354	1.279	5.5	1.352	0.1	1.334	1.5
116-119 Out	1.424	1.275	10.5	1.361	4.4	1.333	6.4

The IEEE 300-bus system is heavily loaded with large number of lines (410 lines), most of the simulated outages either resulted in a voltage collapse or minor negligible effect. The second derivative method provided the least error for all the tested cases in this system. The maximum error is 4.4% in the case of line 116-119 outage. By comparison the linear method had an error of 10.5% and $a = V_0$ approximation method's error was 6.4% for that outage. Table 4.10 provides a statistical analysis of all three methods performance for this system.

Table 4.10 Statistical Analysis of Methods Performance for the IEEE 118-bus System Without Considering Reactive Limits

Method	Linear	Second Derivative	$a = V_0$
Mean Error	8.3	2.5	3.9
Standard Deviation	2.4	1.9	2.5
Max Error	11.0	4.4	6.4
Min Error	5.5	0.1	1.4

4.3 Tests With Generators' Reactive Limits

In these tests, the generator reactive limits were monitored and taken into consideration when calculating proximity to voltage collapse. The following sections discuss the results obtained with reactive limits constraints for the IEEE 14, 57 and 300-bus systems.

4.3.1 Testing the Methods on the IEEE 14-bus System

Similar to the previous section, different outages were performed in this system and the three methods were used to predict the voltage collapse point. Table 4.11 summarizes the results obtained from the simulation.

Table 4.11 Comparison Between the New Methods and the Linear Method for the IEEE 14-bus System While Considering Reactive Limits

Case	λ_m (Actual)	λ_m (Linear Method)	Error (%)	λ_m (Second Derivative Method)	Error (%)	λ_m ($a = V_0$ Method)	Error (%)
Intact	1.766	1.566	11.3	1.741	1.4	1.605	9.1
1-5 Out	1.388	1.235	11.0	1.370	1.3	1.243	10.4
2-3 Out	1.292	1.204	6.8	1.297	-0.4	1.210	6.3
2-4 Out	1.580	1.406	11.0	1.560	1.3	1.431	9.4
2-5 Out	1.649	1.464	11.2	1.627	1.3	1.494	9.4
3-4 Out	1.715	1.559	9.1	1.723	-0.5	1.598	6.8
4-5 Out	1.609	1.445	10.2	1.593	1.0	1.470	8.6
4-7 Out	1.575	1.400	11.1	1.558	1.1	1.412	10.3
4-9 Out	1.676	1.483	11.5	1.652	1.4	1.515	9.6
6-13 Out	1.654	1.428	13.7	1.616	2.3	1.472	11.0
9-14 Out	1.645	1.400	14.9	1.597	2.9	1.446	12.1
12-13 Out	1.764	1.562	11.5	1.738	1.5	1.601	9.2

The results show an enhanced prediction with less errors than the linear method. The second derivative method provided the least error for all the cases displaying a maximum error of 2.9% in the case of line 9-14 outage. By comparison, the linear method had a maximum error of 14.9% and the a = Vo approximation method's maximum error was 12.1% for that outage. Table 4.12 provides a statistical analysis of all three methods performance for this system.

The second derivative prediction was of higher accuracy due to the fact that some generators reached their reactive limits before the prediction point at P-index = 0.5. Moreover, none of the generators reached their reactive limits between that point and the point of collapse.

Table 4.12 Statistical Analysis of Methods Performance for the IEEE 14-bus System While Considering Reactive Limits

Method	Linear	Second Derivative	$a = V_0$
Mean Error	11.1	1.4	9.4
Standard Deviation	1.9	0.7	1.5
Max Error	14.9	2.9	12.1
Min Error	6.8	0.4	6.3

4.3.2 Testing the Methods on the IEEE 57-bus System

The second test system is the IEEE 57-bus system. As before, different outages were performed and the performance of the two proposed methods was examined and compared to the linear method. Table 4.13 summarizes the results of these tests.

Table 4.13 Comparison Between the New Methods and the Linear Method for the IEEE 57-bus System with Considering Reactive Limits

Case	λ_m (Actual)	λ_m (Linear Method)	Error (%)	λ_m (Second Derivative Method)	Error (%)	λ_m ($a = V_0$ Method)	Error (%)
Intact	1.439	1.351	6.1	1.581	-9.9	1.493	-3.8
23-24 Out	1.442	1.307	9.4	1.523	-5.6	1.458	-1.1
13-14 Out	1.451	1.346	7.2	1.573	-8.4	1.491	-2.8
37-38 Out	1.155	1.058	8.4	1.159	-0.3	1.144	1.0
22-38 Out	1.446	1.324	8.4	1.567	-8.4	1.542	-6.6
1-15 Out	1.265	1.175	7.1	1.375	-8.7	1.260	0.4
24-26 Out	1.407	1.238	12.0	1.433	-1.8	1.351	4.0

Unlike the generators in the IEEE 14-bus system, many generators in this system reach their limits between the point of prediction at P-index = 0.5 and the predicted collapse point. This explains the larger errors obtained for this system. Table 4.14 provides a statistical analysis of all three methods performance for this system.

Table 4.14 Statistical Analysis of Methods Performance for the IEEE 57-bus System While Considering Reactive Limits

Method	Linear	Second Derivative	$a = V_0$
Mean Error	8.4	6.2	2.8
Standard Deviation	1.8	3.4	2.0
Max Error	12.0	9.9	6.6
Min Error	6.1	0.3	0.4

4.3.3 Testing the Methods on the IEEE 300-bus System

Similar to the previous test systems, different outages were performed and the performance of the two proposed methods was examined and compared to the linear method. Table 4.15 summarizes the results of these tests.

Table 4.15 Comparison Between the New Methods and the Linear Method for the IEEE 300-bus System with Considering Reactive Limits

Case	λ_m (Actual)	λ_m (Linear Method)	Error (%)	λ_m (Second Derivative Method)	Error (%)	λ_m ($a = V_0$ Method)	Error (%)
Intact	1.058	1.087	-2.7	1.099	-3.9	1.085	-2.6
3-4 Out	1.009	1.058	-4.9	1.069	-5.9	1.065	-5.6
40-68 Out	1.025	1.051	-2.5	1.064	-3.8	1.054	-2.8

The IEEE 300-bus system is heavily stressed with a small margin of loadability. Moreover, similar to the IEEE 57-bus system, many generators reached their reactive limits between the prediction point at P-index=0.5 and the point of collapse leading to inaccuracies in prediction. Table 4.16 provides a statistical analysis of all three methods performance for this system.

Table 4.16 Statistical Analysis of Methods Performance for the IEEE 300-bus System While Considering Reactive Limits

Method	Linear	Second Derivative	$a = V_0$
Mean Error	3.4	4.5	3.6
Standard Deviation	1.0	1.0	1.4
Max Error	4.9	5.9	5.6
Min Error	2.5	3.8	2.6

4.4 Performance Comparison to the Direct Computation Method

The new methods were compared to the direct computation method discussed in section 2.5. All methods times were measured from the system condition at P-index = 0.5. Tables 4.17 and 4.18 provide a performance (only between 2nd Derivative and direct) and time comparison between the different approaches when neglecting reactive limits. While Tables 4.19 and 4.20 provide the same comparison when taking the reactive power limits into consideration.

Table 4.17 Comparison Between the Second Derivative Method and the Direct Computation Method Prediction When Neglecting Reactive Power Limits

System/Method	λ_m (Actual)	λ_m (Second Derivative Method)	Error (%)	λ_m (Direct Computation Method)	Error (%)
IEEE 14-bus	4.040	4.174	-3.317	4.027	0.322
IEEE 39-bus	2.300	2.279	0.913	2.300	0.000
IEEE 57-bus	2.070	1.981	4.300	2.071	-0.048
IEEE 118-bus	3.200	3.262	-1.937	3.185	0.469
IEEE 300-bus	1.430	1.445	-1.049	1.439	-0.629

Table 4.18 Time Comparison Between the Different Approaches When Neglecting Reactive Power Limits

System/Method	Linear (s)	Second Derivative (s)	$a = V_0$ (s)	Direct Computation (s)
IEEE 14-bus	0	0.062	0.016	0.000
IEEE 39-bus	0	0.125	0.031	0.031
IEEE 57-bus	0	0.094	0.031	0.328
IEEE 118-bus	0	0.172	0.031	0.562
IEEE 300-bus	0	0.296	0.094	4.524

Table 4.19 Comparison Between the Second Derivative Method and The Direct Computation Method Prediction When Considering Reactive Power Limits

System/Method	λ_m (Actual)	λ_m (Second Derivative Method)	Error (%)	λ_m (Direct Computation Method)	Error (%)
IEEE 14-bus	1.766	1.741	1.416	1.739	1.546
IEEE 57-bus	1.439	1.581	-9.868	1.569	-9.062
IEEE 300-bus	1.058	1.099	-3.875	1.021	3.497

Table 4.20 Time Comparison Between the Different Approaches When Considering Reactive Power Limits

System/Method	Linear (s)	Second Derivative (s)	$a = V_0$ (s)	Direct Computation (s)
IEEE 14-bus	0	0.078	0.016	0.047
IEEE 57-bus	0	0.14	0.031	0.515
IEEE 300-bus	0	0.39	0.172	69.966

The results of these test show that the linear method is extremely fast. This is due to the calculation approach used in the linear method where one simple arithmetic operation is performed to predict the voltage collapse point [21]. However, the accuracy of this method is low compared to the new proposed methods.

One the other hand, the direct computation method exhibits the highest accuracy (less than 1%) for all the systems when neglecting the reactive power limits. However, the time required to perform the prediction increases significantly as the number of buses increase. This method becomes impractical for online monitoring of large systems. The new methods on the other hand are remarkably faster than the direct computation method, and the accuracy of the second derivative method is comparable to the latter.

When taking the reactive power limits into consideration, both methods, shown on table 4.19, provided approximately similar prediction. However, time comparison between the two demonstrates the enormous gap in speed.

CHAPTER 5

CONCLUSION AND FUTURE WORK

5.1 Conclusion

In this study, an improvement was made to the linear method for voltage collapse point prediction and two new methods were proposed. These took into consideration the assumptions that were carried out in the linear approximation. The new proposed methods provided a better estimation of voltage collapse point compared to the original linear method. Furthermore, the new methods provided high speed of performance.

The performance of the new methods was first investigated on the IEEE 14, 39, 57, 118, and 300-bus system without taking reactive generators limits into consideration. Results of these tests were compared to the original linear approximation method. It was evident that the new methods provided a significant enhancement in estimation of the voltage collapse point.

Next, tests were made on the IEEE 14, 57, and 300-bus systems while taking reactive power limits into consideration. The reactive power limits were monitored until the point of estimation. Results show that the new methods provided better performance when none of the generators hit their limits between the point of estimation and the point of collapse. If generators hit their limits between these two points, all methods showed inaccuracies.

The new methods were also compared to a novel method that used direct computation to predict voltage collapse. This method features precision when neglecting reactive power limits. However, the main drawback is the slow prediction for systems with large number of buses. The

second derivative method that was proposed in this work showed comparable precision and significantly higher speed of estimation.

5.2 Future Work

The first area of recommended research is the modeling of reactive power limits behavior with increased load. The new methods need further investigation in the cases where generators reach their limits between the point of estimation and the point of collapse. If an accurate model that characterizes generator reactive limit behavior is introduced, the new proposed methods would provide significantly higher accuracies.

The second area of recommended research is to explore calculating the exact voltage collapse point using continuation power flow. This can be done by using the predicted system conditions at the collapse point as the starting point for continuation power flow program. Then, performing predictor and corrector steps described in section 2.2 can lead to the exact voltage collapse point.

REFERENCES

[1] P. Kundur, N. J. Balu, and M. G. Lauby, "Voltage stability," in *Power System Stability and Control*. New York: McGraw-Hill, 1994, pp. xxiii, 1176 p.

[2] N. S. Group, "Technical analysis of the August 14, 2003, blackout: what happened, why, and what did we learn," 2004.

[3] US-Canada Power System Outage Task Force, "Power failure in Eastern Denmark and Southern Sweden on 23 September 2003 final report on the course of events," 2004.

[4] J. M. O. Filho, "Brazilian blackout 2009," *PAC World Magazine, pp.* 36-37, March 2010.

[5] M. B. Keskin, "Continuation power flow and voltage stability in power systems," M.S. thesis, EEE Dept., METU Univ., Ankara, Turkey, 2007.

[6] B. Gao, G. Morison, and P. Kundur, "Voltage stability evaluation using modal analysis," *IEEE transactions on power systems,* vol. 7, no. 4, pp. 1529-1542, 1992.

[7] C. E. D. Cardet, "Analysis on voltage stability indices," M.S. thesis, ETSEIB, UPC Univ., Barcelona, Spain, 2010.

[8] P. Lof, T. Smed, G. Andersson, and D. J. Hill, "Fast calculation of a voltage stability index," *IEEE Transactions on Power Systems,* vol. 7, no. 1, pp. 54-64, 1992.

[9] H.-D. Chiang and R. Jean-Jumeau, "Toward a practical performance index for predicting voltage collapse in electric power systems," *IEEE Transactions on power systems,* vol. 10, no. 2, pp. 584-592, 1995.

[10] A. Berizzi, P. Finazzi, D. Dosi, P. Marannino, and S. Corsi, "First and second order methods for voltage collapse assessment and security enhancement," *IEEE Power Engineering Review,* vol. 17, no. 4, pp. 51-51, 1997.

[11] A. Z. De Souza, C. A. Canizares, and V. H. Quintana, "New techniques to speed up voltage collapse computations using tangent vectors," *IEEE Transactions on Power Systems,* vol. 12, no. 3, pp. 1380-1387, 1997.

[12] N. D. Hatziargyriou, J. van Hecke, T. van Cutsem, "Indices predicting voltage collapse including dynamic phenomena,*"* CIGRE, 1994.

[13] M. Moghavvemi and G. Jasmon, "New method for indicating voltage stability condition in power system," in *Proc. Third Int. Power Engineering Conf.,* Singapore, 1997, vol. 1, pp. 223-227.

[14] N.-s. Hang, T. Xu, Q.-h. Liao, and Z.-q. Lu, "The analysis of abundance index of voltage stability based circuit theory," in *Guangxi Electric Power,* 2006, vol. 2, p. 002.

[15] A. Mohamed, G. Jasmon, and S. Yusoff, "A static voltage collapse indicator using line stability factors," *Journal of Industrial Technology,* vol. 7, no. 1, pp. 73-85, 1989.

[16] I. Musirin and T. K. Abdul Rahman, "Novel fast voltage stability index (FVSI) for voltage stability analysis in power transmission system," *Student Conf. on Research and Development,* Shah Alam, Malaysia, 2002, pp. 265-268.

[17] M. Moghavvemi and O. Faruque, "Real-time contingency evaluation and ranking technique," *IEE Proceedings-Generation, Transmission and Distribution,* vol. 145, no. 5, pp. 517-524, 1998.

[18] P. Kessel and H. Glavitsch, "Estimating the voltage stability of a power system," *IEEE Transactions on Power Delivery,* vol. 1, no. 3, pp. 346-354, 1986.

[19] M. H. Haque, "Use of local information to determine the distance to voltage collapse," in *Int. Power Engineering Conf.*, Singapore, 2007, pp. 407-412.

[20] U. Eminoglu and M. H. Hocaoglu, "A voltage stability index for radial distribution networks," in *42nd Int. Universities Power Engineering Conf.*, Brighton, 2007, pp. 408-413.

[21] M. Kamel, A. A. Karrar, and A. H. Eltom, "Development and application of a new voltage stability index for on-line monitoring and shedding," *IEEE Transactions on Power Systems,* vol. 33, no. 2, pp. 1231-1241, 2018.

[22] W. E. Elballa, "A novel optimization formulation for the direct computation of the voltage collapse point," M.S. thesis, EE Dept., UTC Univ., Chattanooga, TN, 2018.

APPENDIX A

JACOBIAN MATRIX EQUATIONS

The Jacobian matrix J can be represented as four submatrices:

$$J = \begin{bmatrix} \frac{\partial P_i}{\partial \delta_k} & \frac{\partial P_i}{\partial V_k} \\ \frac{\partial Q_i}{\partial \delta_k} & \frac{\partial Q_i}{\partial V_k} \end{bmatrix} \quad \text{A.1}$$

The active and reactive power equations are:

$$P_l = \sum_{k=1}^{n} Y_{lk} V_l V_k \cos(\theta_{lk} + \delta_k - \delta_l) \quad \text{A.2}$$

$$Q_l = -\sum_{k=1}^{n} Y_{lk} V_l V_k \sin(\theta_{lk} + \delta_k - \delta_l) \quad \text{A.3}$$

There are two cases for each submatrix of the Jacobian matrix. For the first submatrix:

$$\left.\frac{\partial P_l}{\partial \delta_k}\right|_{l \neq k} = -Y_{lk} V_l V_k \sin(\theta_{lk} + \delta_k - \delta_l) \quad \text{A.4}$$

$$\left.\frac{\partial P_l}{\partial \delta_k}\right|_{l = k} = \sum_{\substack{k=1 \\ k \neq l}}^{n} Y_{lk} V_l V_k \sin(\theta_{lk} + \delta_k - \delta_l) = -Q_l - Y_{ll} V_l^2 \sin(\theta_{ll}) \quad \text{A.5}$$

As for the second submatrix:

$$\left.\frac{\partial P_l}{\partial V_k}\right|_{l \neq k} = Y_{lk} V_l \cos(\theta_{lk} + \delta_k - \delta_l) \quad \text{A.6}$$

$$\left.\frac{\partial P_l}{\partial V_k}\right|_{l = k} = \sum_{\substack{k=1 \\ k \neq l}}^{n} Y_{lk} V_k \cos(\theta_{lk} + \delta_k - \delta_l) + 2 Y_{ll} V_l \cos(\theta_{ll}) \quad \text{A.7}$$

$$= \frac{P_l}{V_l} + Y_{ll} V_l \cos(\theta_{ll})$$

As for the third submatrix:

$$\left.\frac{\partial Q_l}{\partial \delta_k}\right|_{l \neq k} = -Y_{lk} V_l V_k \cos(\theta_{lk} + \delta_k - \delta_l) \quad \text{A.8}$$

$$\left.\frac{\partial Q_l}{\partial \delta_k}\right|_{l=k} = \sum_{\substack{k=1 \\ k \neq l}}^{n} Y_{lk} V_l V_k \cos(\theta_{lk} + \delta_k - \delta_l) + 2 Y_{ll} V_l \cos(\theta_{ll}) \quad \text{A.9}$$

$$= P_l - Y_{ll} V_l^2 \cos(\theta_{ll})$$

As for the fourth submatrix:

$$\left.\frac{\partial Q_l}{\partial V_k}\right|_{l \neq k} = -Y_{lk} V_l \sin(\theta_{lk} + \delta_k - \delta_l) \quad \text{A.10}$$

$$\left.\frac{\partial Q_l}{\partial V_k}\right|_{l=k} = -\sum_{\substack{k=1 \\ k \neq l}}^{n} Y_{lk} V_k \sin(\theta_{lk} + \delta_k - \delta_l) - 2 Y_{ll} V_l \sin(\theta_{ll}) \quad \text{A.11}$$

$$= \frac{Q_l}{V_l} - Y_{ll} V_l \sin(\theta_{ll})$$

APPENDIX B

HESSIAN MATRIX FORMULATION

The Hessian matrix shown in equation 3.39 can be divided into four submatrices:

$$H = \begin{bmatrix} H_{11} & H_{12} \\ H_{21} & H_{22} \end{bmatrix} \tag{A.12}$$

The 1st submatrix is:

$$H_{11} = \begin{bmatrix} \frac{d}{dP_i}\left(\frac{\partial P_1}{\partial \delta_1}\right) & \cdots & \frac{d}{dP_i}\left(\frac{\partial P_1}{\partial \delta_i}\right) & \cdots & \frac{d}{dP_i}\left(\frac{\partial P_1}{\partial \delta_n}\right) \\ \vdots & \ddots & \vdots & \ddots & \vdots \\ \frac{d}{dP_i}\left(\frac{\partial P_i}{\partial \delta_1}\right) & \cdots & \frac{d}{dP_i}\left(\frac{\partial P_i}{\partial \delta_i}\right) & \cdots & \frac{d}{dP_i}\left(\frac{\partial P_i}{\partial \delta_n}\right) \\ \vdots & \ddots & \vdots & \ddots & \vdots \\ \frac{d}{dP_i}\left(\frac{\partial P_n}{\partial \delta_1}\right) & \cdots & \frac{d}{dP_i}\left(\frac{\partial P_n}{\partial \delta_i}\right) & \cdots & \frac{d}{dP_i}\left(\frac{\partial P_n}{\partial \delta_n}\right) \end{bmatrix} \tag{A.13}$$

Expanding the first element:

$$\frac{d}{dP_i}\left(\frac{\partial P_1}{\partial \delta_1}\right) = \frac{\partial^2 P_1}{\partial \delta_1 \partial \delta_1}\frac{d\delta_1}{dP_i} + \cdots + \frac{\partial^2 P_1}{\partial \delta_j \partial \delta_1}\frac{d\delta_j}{dP_i} + \cdots + \frac{\partial^2 P_1}{\partial \delta_n \partial \delta_1}\frac{d\delta_n}{dP_i} + \cdots + \frac{\partial^2 P_1}{\partial V_1 \partial \delta_1}\frac{dV_1}{dP_i} + \cdots + \frac{\partial^2 P_1}{\partial V_j \partial \delta_1}\frac{dV_j}{dP_i} + \cdots + \frac{\partial^2 P_1}{\partial V_n \partial \delta_1}\frac{dV_n}{dP_i} \tag{A.14}$$

And, for the l^{th} bus

$$\frac{d}{dP_i}\left(\frac{\partial P_l}{\partial \delta_k}\right) = \frac{\partial^2 P_l}{\partial \delta_1 \partial \delta_k}\frac{d\delta_1}{dP_i} + \cdots + \frac{\partial^2 P_l}{\partial \delta_j \partial \delta_k}\frac{d\delta_j}{dP_i} + \cdots + \frac{\partial^2 P_l}{\partial \delta_n \partial \delta_k}\frac{d\delta_n}{dP_i} + \cdots + \frac{\partial^2 P_l}{\partial V_1 \partial \delta_k}\frac{dV_1}{dP_i} + \cdots + \frac{\partial^2 P_l}{\partial V_j \partial \delta_k}\frac{dV_j}{dP_i} + \cdots + \frac{\partial^2 P_l}{\partial V_n \partial \delta_k}\frac{dV_n}{dP_i} \tag{A.15}$$

Or, in general:

$$\frac{d}{dP_i}\left(\frac{\partial P_l}{\partial \delta_k}\right) = \cdots + \frac{\partial^2 P_l}{\partial \delta_j \partial \delta_k}\frac{d\delta_j}{dP_i} + \cdots + \frac{\partial^2 P_l}{\partial V_j \partial \delta_k}\frac{dV_j}{dP_i} + \cdots \qquad \text{A.16}$$

These derivatives are derived from the Jacobian matrix equations.

Now consider the first group of terms in A.16, $(\frac{\partial^2 P_l}{\partial \delta_j \partial \delta_k}\frac{d\delta_j}{dP_i})$. There are five combinations for l, k and j for this term:

$$\frac{\partial}{\partial \delta_j}\left(\frac{\partial P_l}{\partial \delta_k}\right)\Bigg|_{l\neq k\neq j} = 0 \qquad \text{A.17}$$

$$\frac{\partial}{\partial \delta_j}\left(\frac{\partial P_l}{\partial \delta_k}\right)\Bigg|_{l\neq k=j} = -Y_{lk}V_lV_k\cos(\theta_{lk}+\delta_k-\delta_l) = J_{21}(l,k) \qquad \text{A.18}$$

$$\frac{\partial}{\partial \delta_j}\left(\frac{\partial P_l}{\partial \delta_k}\right)\Bigg|_{l=j\neq k} = Y_{lk}V_lV_k\cos(\theta_{lk}+\delta_k-\delta_l) = -J_{21}(l,k) \qquad \text{A.19}$$

$$\frac{\partial}{\partial \delta_j}\left(\frac{\partial P_l}{\partial \delta_k}\right)\Bigg|_{l=k\neq j} = Y_{lj}V_lV_j\cos\left(\theta_{lj}+\delta_j-\delta_l\right) = -J_{21}(l,j) \qquad \text{A.20}$$

$$\frac{\partial}{\partial \delta_j}\left(\frac{\partial P_l}{\partial \delta_k}\right)\Bigg|_{l=k=j} = -\sum_{\substack{k=1\\k\neq l}}^{n} Y_{lk}V_lV_k\cos(\theta_{lk}+\delta_k-\delta_l) \qquad \text{A.21}$$

$$= -P_l + Y_{ll}V_l^2\cos(\theta_{ll}) = -J_{21}(l,l)$$

The same five cases apply for the second group of terms ($\frac{\partial^2 P_l}{\partial V_j \partial \delta_k}\frac{dV_j}{dP_i}$):

$$\frac{\partial}{\partial V_j}\left(\frac{\partial P_l}{\partial \delta_k}\right)\Big|_{l\neq k\neq j} = 0 \tag{A.22}$$

$$\frac{\partial}{\partial V_j}\left(\frac{\partial P_l}{\partial \delta_k}\right)\Big|_{l\neq k=j} = -Y_{lk}V_l\sin(\theta_{lk}+\delta_k-\delta_l) = J_{22}(l,k) \tag{A.23}$$

$$\frac{\partial}{\partial V_j}\left(\frac{\partial P_l}{\partial \delta_k}\right)\Big|_{l=j\neq k} = -Y_{lk}V_k\sin(\theta_{lk}+\delta_k-\delta_l) = J_{22}(l,k)\cdot\frac{V_k}{V_i} \tag{A.24}$$

$$\frac{\partial}{\partial V_j}\left(\frac{\partial P_l}{\partial \delta_k}\right)\Big|_{l=k\neq j} = Y_{lj}V_l\sin\left(\theta_{lj}+\delta_j-\delta_l\right) = -J_{22}(l,j) \tag{A.25}$$

$$\begin{aligned}\frac{\partial}{\partial V_j}\left(\frac{\partial P_l}{\partial \delta_k}\right)\Big|_{l=k=j} &= \sum_{\substack{k=1\\k\neq l}}^{n} Y_{lk}V_k\sin(\theta_{lk}+\delta_k-\delta_l)\\ &= -\frac{Q_l}{V_l} - Y_{ll}V_l\sin(\theta_{ll}) = J_{11}(l,l)\cdot\frac{1}{V_l}\end{aligned} \tag{A.26}$$

Now moving to the 2nd submatrix of the Hessian:

$$H_{12} = \begin{bmatrix} \frac{d}{dP_i}\left(\frac{\partial P_1}{\partial V_1}\right) & \cdots & \frac{d}{dP_i}\left(\frac{\partial P_1}{\partial V_i}\right) & \cdots & \frac{d}{dP_i}\left(\frac{\partial P_1}{\partial V_n}\right) \\ \vdots & \ddots & \vdots & \ddots & \vdots \\ \frac{d}{dP_i}\left(\frac{\partial P_i}{\partial V_1}\right) & \cdots & \frac{d}{dP_i}\left(\frac{\partial P_i}{\partial V_i}\right) & \cdots & \frac{d}{dP_i}\left(\frac{\partial P_i}{\partial V_n}\right) \\ \vdots & \ddots & \vdots & \ddots & \vdots \\ \frac{d}{dP_i}\left(\frac{\partial P_n}{\partial V_1}\right) & \cdots & \frac{d}{dP_i}\left(\frac{\partial P_n}{\partial V_i}\right) & \cdots & \frac{d}{dP_i}\left(\frac{\partial P_n}{\partial V_n}\right) \end{bmatrix} \tag{A.27}$$

Expanding the first element:

$$\frac{d}{dP_i}\left(\frac{\partial P_1}{\partial V_1}\right) = \frac{\partial^2 P_1}{\partial \delta_1 \partial V_1}\frac{d\delta_1}{dP_i} + \cdots + \frac{\partial^2 P_1}{\partial \delta_j \partial V_1}\frac{d\delta_j}{dP_i} + \cdots + \frac{\partial^2 P_1}{\partial \delta_n \partial V_1}\frac{d\delta_n}{dP_i} + \cdots + \frac{\partial^2 P_1}{\partial V_1 \partial V_1}\frac{dV_1}{dP_i} + \cdots + \frac{\partial^2 P_1}{\partial V_j \partial V_1}\frac{dV_j}{dP_i} + \cdots + \frac{\partial^2 P_1}{\partial V_n \partial V_1}\frac{dV_n}{dP_i} \quad \text{A.28}$$

And, for the l^{th} bus:

$$\frac{d}{dP_i}\left(\frac{\partial P_l}{\partial V_k}\right) = \frac{\partial^2 P_l}{\partial \delta_1 \partial V_k}\frac{d\delta_1}{dP_i} + \cdots + \frac{\partial^2 P_l}{\partial \delta_j \partial V_k}\frac{d\delta_j}{dP_i} + \cdots + \frac{\partial^2 P_l}{\partial \delta_n \partial V_k}\frac{d\delta_n}{dP_i} + \cdots + \frac{\partial^2 P_l}{\partial V_1 \partial V_k}\frac{dV_1}{dP_i} + \cdots + \frac{\partial^2 P_l}{\partial V_j \partial V_k}\frac{dV_j}{dP_i} + \cdots + \frac{\partial^2 P_l}{\partial V_n \partial V_k}\frac{dV_n}{dP_i} \quad \text{A.29}$$

Or, in general:

$$\frac{d}{dP_i}\left(\frac{\partial P_l}{\partial V_k}\right) = \cdots + \frac{\partial^2 P_l}{\partial \delta_j \partial V_k}\frac{d\delta_j}{dP_i} + \cdots + \frac{\partial^2 P_l}{\partial V_j \partial V_k}\frac{dV_j}{dP_i} + \cdots \quad \text{A.30}$$

Again, there are five cases for l, k and j for the first group of terms ($\frac{\partial^2 P_l}{\partial \delta_j \partial V_k}\frac{d\delta_j}{dP_i}$):

$$\frac{\partial}{\partial \delta_j}\left(\frac{\partial P_l}{\partial V_k}\right)\Bigg|_{l\neq k\neq j} = 0 \quad \text{A.31}$$

$$\frac{\partial}{\partial \delta_j}\left(\frac{\partial P_l}{\partial V_k}\right)\Bigg|_{l\neq k= j} = -Y_{lk}V_l \sin(\theta_{lk} + \delta_k - \delta_l) = J_{22}(l,k) \quad \text{A.32}$$

$$\frac{\partial}{\partial \delta_j}\left(\frac{\partial P_l}{\partial V_k}\right)\Bigg|_{l= j\neq k} = Y_{lk}V_l \sin(\theta_{lk} + \delta_k - \delta_l) = -J_{22}(l,k) \quad \text{A.33}$$

$$\frac{\partial}{\partial \delta_j}\left(\frac{\partial P_l}{\partial V_k}\right)\Bigg|_{l= k\neq j} = -Y_{lj}V_j \sin\left(\theta_{lj} + \delta_j - \delta_l\right) = J_{22}(l,j)\cdot\frac{V_j}{V_l} \quad \text{A.34}$$

$$\left.\frac{\partial}{\partial \delta_j}\left(\frac{\partial P_l}{\partial V_k}\right)\right|_{l=k=j} = \sum_{\substack{k=1 \\ k\neq l}}^{n} Y_{lk} V_k \sin(\theta_{lk} + \delta_k - \delta_l)$$

$$= -\frac{Q_l}{V_l} - Y_{ll} V_l \sin(\theta_{ll}) = J_{11}(l,l) \cdot \frac{1}{V_l} \qquad \text{A.35}$$

As for the second group ($\frac{\partial^2 P_l}{\partial V_j V_k}\frac{dV_j}{dP_i}$):

$$\left.\frac{\partial}{\partial V_j}\left(\frac{\partial P_l}{\partial V_k}\right)\right|_{l\neq k\neq j} = 0 \qquad \text{A.36}$$

$$\left.\frac{\partial}{\partial V_j}\left(\frac{\partial P_l}{\partial V_k}\right)\right|_{l\neq k=j} = 0 \qquad \text{A.37}$$

$$\left.\frac{\partial}{\partial V_j}\left(\frac{\partial P_l}{\partial V_k}\right)\right|_{l=j\neq k} = Y_{lk} \cos(\theta_{lk} + \delta_k - \delta_l) = J_{12}(l,k) \cdot \frac{1}{V_l} \qquad \text{A.38}$$

$$\left.\frac{\partial}{\partial V_j}\left(\frac{\partial P_l}{\partial V_k}\right)\right|_{l=k\neq j} = Y_{lj} \cos\left(\theta_{lj} + \delta_j - \delta_l\right) = J_{12}(l,j) \cdot \frac{1}{V_l} \qquad \text{A.39}$$

$$\left.\frac{\partial}{\partial V_j}\left(\frac{\partial P_l}{\partial V_k}\right)\right|_{l=k=j} = 2Y_{ll} \cos(\theta_{ll}) = J_{12}(l,l) \cdot \frac{1}{V_l} - J_{21}(l,l) \cdot \frac{1}{V_l^2} \qquad \text{A.40}$$

The 3rd submatrix is:

$$H_{21} = \begin{bmatrix} \frac{d}{dP_i}\left(\frac{\partial Q_1}{\partial \delta_1}\right) & \cdots & \frac{d}{dP_i}\left(\frac{\partial Q_1}{\partial \delta_i}\right) & \cdots & \frac{d}{dP_i}\left(\frac{\partial Q_1}{\partial \delta_n}\right) \\ \vdots & \ddots & \vdots & \ddots & \vdots \\ \frac{d}{dP_i}\left(\frac{\partial Q_i}{\partial \delta_1}\right) & \cdots & \frac{d}{dP_i}\left(\frac{\partial Q_i}{\partial \delta_i}\right) & \cdots & \frac{d}{dP_i}\left(\frac{\partial Q_i}{\partial \delta_n}\right) \\ \vdots & \ddots & \vdots & \ddots & \vdots \\ \frac{d}{dP_i}\left(\frac{\partial Q_n}{\partial \delta_1}\right) & \cdots & \frac{d}{dP_i}\left(\frac{\partial Q_n}{\partial \delta_i}\right) & \cdots & \frac{d}{dP_i}\left(\frac{\partial Q_n}{\partial \delta_n}\right) \end{bmatrix} \quad \text{A.41}$$

Expanding the first element:

$$\frac{d}{dP_i}\left(\frac{\partial Q_1}{\partial \delta_1}\right) = \frac{\partial^2 Q_1}{\partial \delta_1 \partial \delta_1}\frac{d\delta_1}{dP_i} + \cdots + \frac{\partial^2 Q_1}{\partial \delta_j \partial \delta_1}\frac{d\delta_j}{dP_i} + \cdots + \frac{\partial^2 Q_1}{\partial \delta_n \partial \delta_1}\frac{d\delta_n}{dP_i} + \cdots + \frac{\partial^2 Q_1}{\partial V_1 \partial \delta_1}\frac{dV_1}{dP_i} + \cdots + \frac{\partial^2 Q_1}{\partial V_j \partial \delta_1}\frac{dV_j}{dP_i} + \cdots + \frac{\partial^2 Q_1}{\partial V_n \partial \delta_1}\frac{dV_n}{dP_i} \quad \text{A.42}$$

And, for the l^{th} bus:

$$\frac{d}{dP_i}\left(\frac{\partial Q_l}{\partial \delta_k}\right) = \frac{\partial^2 Q_l}{\partial \delta_1 \partial \delta_k}\frac{d\delta_1}{dP_i} + \cdots + \frac{\partial^2 Q_l}{\partial \delta_j \partial \delta_k}\frac{d\delta_j}{dP_i} + \cdots + \frac{\partial^2 Q_l}{\partial \delta_n \partial \delta_k}\frac{d\delta_n}{dP_i} + \cdots + \frac{\partial^2 Q_l}{\partial V_1 \partial \delta_k}\frac{dV_1}{dP_i} + \cdots + \frac{\partial^2 Q_l}{\partial V_j \partial \delta_k}\frac{dV_j}{dP_i} + \cdots + \frac{\partial^2 Q_l}{\partial V_n \partial \delta_k}\frac{dV_n}{dP_i} \quad \text{A.43}$$

Or, in general:

$$\frac{d}{dP_i}\left(\frac{\partial Q_l}{\partial \delta_k}\right) = \cdots + \frac{\partial^2 Q_l}{\partial \delta_j \partial \delta_k}\frac{d\delta_j}{dP_i} + \cdots + \frac{\partial^2 Q_l}{\partial V_j \partial \delta_k}\frac{dV_j}{dP_i} + \cdots \quad \text{A.44}$$

The five cases for the first group of terms ($\frac{\partial^2 Q_l}{\partial \delta_j \partial \delta_k}\frac{d\delta_j}{dP_i}$) are:

$$\frac{\partial}{\partial \delta_j}\left(\frac{\partial Q_l}{\partial \delta_k}\right)\Big|_{l\neq k\neq j} = 0 \tag{A.45}$$

$$\frac{\partial}{\partial \delta_j}\left(\frac{\partial Q_l}{\partial \delta_k}\right)\Big|_{l\neq k=j} = Y_{lk}V_lV_k\sin(\theta_{lk}+\delta_k-\delta_l) = -J_{11}(l,k) \tag{A.46}$$

$$\frac{\partial}{\partial \delta_j}\left(\frac{\partial Q_l}{\partial \delta_k}\right)\Big|_{l=j\neq k} = -Y_{lk}V_lV_k\sin(\theta_{lk}+\delta_k-\delta_l) = J_{11}(l,k) \tag{A.47}$$

$$\frac{\partial}{\partial \delta_j}\left(\frac{\partial Q_l}{\partial \delta_k}\right)\Big|_{l=k\neq j} = -Y_{lj}V_lV_j\sin\left(\theta_{lj}+\delta_j-\delta_l\right) = J_{11}(l,j) \tag{A.48}$$

$$\begin{aligned}\frac{\partial}{\partial \delta_j}\left(\frac{\partial Q_l}{\partial \delta_k}\right)\Big|_{l=k=j} &= \sum_{\substack{k=1\\k\neq l}}^{n} Y_{lk}V_lV_k\sin(\theta_{lk}+\delta_k-\delta_l)\\ &= -Q_l + Y_{ll}V_l^2\sin(\theta_{ll}) = J_{11}(l,l)\end{aligned} \tag{A.49}$$

As for the second group of terms ($\frac{\partial^2 Q_l}{\partial V_j \partial \delta_k}\frac{dV_j}{dP_i}$)

$$\frac{\partial}{\partial V_j}\left(\frac{\partial Q}{\partial \delta_k}\right)\Big|_{l\neq k\neq j} = 0 \tag{A.50}$$

$$\frac{\partial}{\partial V_j}\left(\frac{\partial Q}{\partial \delta_k}\right)\Big|_{l\neq k=j} = -Y_{lk}V_l\cos(\theta_{lk}+\delta_k-\delta_l) = -J_{12}(l,k) \tag{A.51}$$

$$\frac{\partial}{\partial V_j}\left(\frac{\partial Q}{\partial \delta_k}\right)\Big|_{l=j\neq k} = -Y_{lk}V_k\cos(\theta_{lk}+\delta_k-\delta_l) = -J_{12}(l,k)\cdot\frac{V_k}{V_i} \tag{A.52}$$

$$\frac{\partial}{\partial V_j}\left(\frac{\partial Q}{\partial \delta_k}\right)\Big|_{l=k\neq j} = Y_{lj}V_l\cos\left(\theta_{lj}+\delta_j-\delta_l\right) = J_{12}(l,j) \tag{A.53}$$

$$\left.\frac{\partial}{\partial V_j}\left(\frac{\partial Q}{\partial \delta_k}\right)\right|_{l=k=j} = \sum_{\substack{k=1 \\ k\neq l}}^{n} Y_{lk}V_k\cos(\theta_{lk}+\delta_k-\delta_l)$$

$$= \frac{P_l}{V_l} - Y_{ll}V_l\cos(\theta_{ll}) = J_{21}(l,l)\cdot\frac{1}{V_l} \qquad \text{A.54}$$

Finally, the 4th submatrix is:

$$H_{22} = \begin{bmatrix} \frac{d}{dP_i}\left(\frac{\partial Q_1}{\partial V_1}\right) & \cdots & \frac{d}{dP_i}\left(\frac{\partial Q_1}{\partial V_i}\right) & \cdots & \frac{d}{dP_i}\left(\frac{\partial Q_1}{\partial V_n}\right) \\ \vdots & \ddots & \vdots & \ddots & \vdots \\ \frac{d}{dP_i}\left(\frac{\partial Q_i}{\partial V_1}\right) & \cdots & \frac{d}{dP_i}\left(\frac{\partial Q_i}{\partial V_i}\right) & \cdots & \frac{d}{dP_i}\left(\frac{\partial Q_i}{\partial V_n}\right) \\ \vdots & \ddots & \vdots & \ddots & \vdots \\ \frac{d}{dP_i}\left(\frac{\partial Q_n}{\partial V_1}\right) & \cdots & \frac{d}{dP_i}\left(\frac{\partial Q_n}{\partial V_i}\right) & \cdots & \frac{d}{dP_i}\left(\frac{\partial Q_n}{\partial V_n}\right) \end{bmatrix} \qquad \text{A.55}$$

Expanding the first element:

$$\frac{d}{dP_i}\left(\frac{\partial Q_1}{\partial V_1}\right) = \frac{\partial^2 Q_1}{\partial\delta_1\partial V_1}\frac{d\delta_1}{dP_i} + \cdots + \frac{\partial^2 Q_1}{\partial\delta_j\partial V_1}\frac{d\delta_j}{dP_i} + \cdots + \frac{\partial^2 Q_1}{\partial\delta_n\partial V_1}\frac{d\delta_n}{dP_i}$$

$$+ \cdots + \frac{\partial^2 Q_1}{\partial V_1\partial V_1}\frac{dV_1}{dP_i} + \cdots + \frac{\partial^2 Q_1}{\partial V_j\partial V_1}\frac{dV_j}{dP_i} + \cdots + \frac{\partial^2 Q_1}{\partial V_n\partial V_1}\frac{dV_n}{dP_i} \qquad \text{A.56}$$

And, in general, for the l^{th} bus:

$$\frac{d}{dP_i}\left(\frac{\partial Q_l}{\partial V_k}\right) = \frac{\partial^2 Q_l}{\partial\delta_1\partial V_k}\frac{d\delta_1}{dP_i} + \cdots + \frac{\partial^2 Q_l}{\partial\delta_j\partial V_k}\frac{d\delta_j}{dP_i} + \cdots + \frac{\partial^2 Q_l}{\partial\delta_n\partial V_k}\frac{d\delta_n}{dP_i}$$

$$+ \cdots + \frac{\partial^2 Q_l}{\partial V_1\partial V_k}\frac{dV_1}{dP_i} + \cdots + \frac{\partial^2 Q_l}{\partial V_j\partial V_k}\frac{dV_j}{dP_i} + \cdots + \frac{\partial^2 Q_l}{\partial V_n\partial V_k}\frac{dV_n}{dP_i} \qquad \text{A.57}$$

Or, in short:

$$\frac{d}{dP_i}\left(\frac{\partial Q_l}{\partial V_k}\right) = \cdots + \frac{\partial^2 Q_l}{\partial\delta_j\partial V_k}\frac{d\delta_j}{dP_i} + \cdots + \frac{\partial^2 Q_l}{\partial V_j\partial V_k}\frac{dV_j}{dP_i} + \cdots \qquad \text{A.58}$$

The five cases for the first group of terms ($\frac{\partial^2 Q_l}{\partial \delta_j \partial V_k}\frac{d\delta_j}{dP_i}$) are:

$$\frac{\partial}{\partial \delta_j}\left(\frac{\partial Q_l}{\partial V_k}\right)\Big|_{l\neq k\neq j} = 0 \tag{A.59}$$

$$\frac{\partial}{\partial \delta_j}\left(\frac{\partial Q_l}{\partial V_k}\right)\Big|_{l\neq k=j} = -Y_{lk}V_l\cos(\theta_{lk}+\delta_k-\delta_l) = -J_{12}(l,k) \tag{A.60}$$

$$\frac{\partial}{\partial \delta_j}\left(\frac{\partial Q_l}{\partial V_k}\right)\Big|_{l=j\neq k} = Y_{lk}V_l\cos(\theta_{lk}+\delta_k-\delta_l) = J_{12}(l,k) \tag{A.61}$$

$$\frac{\partial}{\partial \delta_j}\left(\frac{\partial Q_l}{\partial V_k}\right)\Big|_{l=k\neq j} = -Y_{lj}V_j\cos\left(\theta_{lj}+\delta_j-\delta_l\right) = -J_{12}(l,j)\cdot\frac{V_j}{V_i} \tag{A.62}$$

$$\begin{aligned}\frac{\partial}{\partial \delta_j}\left(\frac{\partial Q_l}{\partial V_k}\right)\Big|_{l=k=j} &= \sum_{\substack{k=1\\k\neq l}}^{n} Y_{lk}V_k\cos(\theta_{lk}+\delta_k-\delta_l)\\ &= \frac{P_l}{V_l} - Y_{ll}V_l\cos(\theta_{ll}) = J_{21}(l,l)\cdot\frac{1}{V_l}\end{aligned} \tag{A.63}$$

As for the second group of terms ($\frac{\partial^2 Q_l}{\partial V_j V_k}\frac{dV_j}{dP_i}$):

$$\frac{\partial}{\partial V_j}\left(\frac{\partial Q_l}{\partial V_k}\right)\Big|_{l\neq k\neq j} = 0 \tag{A.64}$$

$$\frac{\partial}{\partial V_j}\left(\frac{\partial Q_l}{\partial V_k}\right)\Big|_{l\neq k=j} = 0 \tag{A.65}$$

$$\frac{\partial}{\partial V_j}\left(\frac{\partial Q_l}{\partial V_k}\right)\Big|_{l=j\neq k} = -Y_{lk}\sin(\theta_{lk}+\delta_k-\delta_l) = J_{22}(l,k)\cdot\frac{1}{V_l} \tag{A.66}$$

$$\frac{\partial}{\partial V_j}\left(\frac{\partial Q_l}{\partial V_k}\right)\Bigg|_{l=k\neq j} = -Y_{lj}\sin\left(\theta_{lj}+\delta_j-\delta_l\right) = J_{22}(l,j)\cdot\frac{1}{V_l} \qquad \text{A.67}$$

$$\frac{\partial}{\partial V_j}\left(\frac{\partial Q_l}{\partial V_k}\right)\Bigg|_{l=k=j} = -2Y_{ll}\sin(\theta_{ll}) = J_{22}(l,l)\cdot\frac{1}{V_l} + J_{11}(l,l)\cdot\frac{1}{V_l^2} \qquad \text{A.68}$$

VITA

Siddig Mohammed was born and raised in El Manaqil, Gezira, Sudan. Before attending The University of Tennessee at Chattanooga as a Master of Science candidate, he attended the University of Khartoum in Khartoum, Sudan, where he earned a Bachelor of Science in Electrical Engineering, First Class, in 2015. In January 2017, Mr. Mohammed was awarded a scholarship and joined The University of Tennessee at Chattanooga as a research assistant. Siddig was awarded a Master of Science degree in Electrical Engineering in December 2018.

While at The University of Tennessee at Chattanooga, Siddig was a member of the College of Engineering and Computer Science Dean's Student Advisory Council. He also presented research at the 2018 CECS Technology Symposium. In addition, Siddig authored an article for the IEEE 2018 PES General Meeting in Portland, Oregon.

Currently, Siddig is working in Chattanooga, Tennessee as an electrical engineer at Mesa Associates Inc.